PEOPLE'S DEMOCRATIC REPUBLIC OF ALGERIA

MINISTRY OF HIGHER EDUCATION AND SCIENTIFIC RESEARCH

UNIVERSITY OF ECHAHID HAMMA LAKHDAR - EL OUED

Faculty of Technology

Laboratory for the Exploitation and Development of Saharan Energy Resources (LEVRES)

Doctoral Thesis

Submitted by:

MOHAMED TAYEB BOUSSABEUR

In order to obtain the **LMD DOCTORATE** degree in:

Option: Electrical control

Entitled

Integration of Z-source Inverter in Electrical Systems

Defended on 28/05/ 2023, before the jury composed of:

Mr. Youcef Bekakra	Professor	University of El Oued	President
Mr. Rabhi Boualaga	Professor	University of Biskra	Supervisor
Mr. Laid Zellouma	Professor	University of El Oued	Co-Supervisor
Mr. Amar Benaissa	Professor	University of Djelfa	Examiner
Mr. Talal Guia	MCA	University of El Oued	Examiner

University Year 2022/2023

REPUBLIQUE ALGERIENNE DEMOCRATIQUE ET POPULAIRE
MINIISTERE DE L'ENSEIGNEMENT SUPERIEUR ET DE LA RECHERCHE SCIENTIFIQUE
UNIVERSITE ECHAHID HAMMA LAKHDAR - EL OUED

Faculté de Technologie

Laboratoire d'Exploitation et de Valorisation des Ressources Energétiques Sahariennes (LEVRES)

Thèse de Doctorat

Présentée par :

MOHAMED TAYEB BOUSSABEUR

En vue de l'obtention du diplôme de **DOCTORAT LMD** en **:**

Option : Commande Electrique

Intitulé

Intégration des convertisseurs Z-source dans les systèmes électriques

Soutenue le 28/ 05/ 2023, devant le jury composé :

Mr. Youcef Bekakra	Professeur	Université d'El Oued	Président
Mr. Rabhi Boualaga	Professeur	Université de Biskra	Rapporteur
Mr. Laid Zellouma	Professeur	Université d'El Oued	Co-Rapporteur
Mr. Amar Benaissa	Professeur	Université de Djelfa	Examinateur
Mr. Talal Guia	MCA	Université d'El Oued	Examinateur

Année Universitaire 2022/2023

ACKNOWLEDGMENT

First of all, I would like to introduce my greatly indebted in my work and success to my Merciful **GOD** who supported me with patience and strength to complete this thesis.

Cordial thanks and deep gratitude are offered to my supervisors **Prof. Rabhi Boualaga** and **Prof.Laid Zellouma** for the patience guidance, encouragement and supervision.

I express my sincere gratitude to the examination committee members: **Prof. Youcef Bekakra**, **Prof. Amar Benaissa**, and **Dr. Talal Guia** for allowing my defense to be a fun experience and for their helpful criticism and recommendations.

Special thanks to staff members and instructors of my department for their exerted efforts to facilitate the difficulties during the work.

Thanks to my parents for always loving and supporting me and for giving me all I needed to do this work.

CONTENTS

List of Tables

List of Figures

NOMENCLATURE

List of abbreviations

RER: Renewable energy resources

PV: Photovoltaic

APS: Autonomous power supply

ZSI: Z-source inverter

ZSFLI: Z-source four-leg inverter

FSMPC: Finite Control Set Model Predictive Control

DER : Distributed Energy Resources

DG: Distributed Generations

LVDC: Low-Voltage DC

VSIs : Voltage-source inverters

MC : Matrix Converter

PMSG : Permanent Magnet Synchronous Generator

PM : Permanent Magnet

THD : Total harmonic distortion

PID : Proportional-integral-derivative

PR : Proportional resonant control

HC : Hysteresis control

SMC: Sliding Mode control

PWM: Pulse width modulation

MPC: Model predictive control

CSI: Current-Source Inverters

UPS: Uninterruptible power supply

ASD: Adjustable speed drives

List of symbols

$R_{p:}$ Parallel resistance

R_s : Series resistance

I : The photovoltaic cell terminal current

V: The photovoltaic cell terminal voltage

L_1, L_2: Inductors of ZSI

C_1, C_2: Capacitors of ZSI

u_L : Inductor voltage of ZSI

u_d: Diode voltage of ZSI

u_i : DC-link voltage of ZSI

U_C : Capacitor voltage of ZSI

E: The DC voltage from the PV panel

T_0 : State shoot-through zero state interval

T_1: State active interval

T: Total interval

U_{i_av}: The average dc-link voltage across the inverter bridge

U_{i_peak} : The peak dc-link voltage across the inverter bridge

B: Boosting factor

S_a, S_b, S_c : Control signals

U_{an}, U_{bn}, U_{cn}: The model four leg inverter's output voltage for each phase

R_{fa}, R_{fb}, R_{fc}: Resistances filter of each phase of the model four leg inverter

L_{fa}, L_{fb}, L_{fc} : Inductors filter of each phase of the model four leg inverter

R_a, R_b, R_c : Loads resistance of each phase of the model four leg inverter

g: Objective function

K: Sampling instant

m: Switching state

T_s: Sampling period

i_c : Capacitor current of ZSI

F: Nominal frequency

i_a, i_b, i_c: Load currents

GENERAL INTRODUCTION

Compared to conventional subterranean fuels, renewable energy resources (RER) such as solar, wind, and geothermal power systems have attracted more attention because of their low production costs and lack of pollution. The photovoltaic (PV) generation system can effectively be employed as an autonomous power supply (APS) for consumers who are geographically located in remote, inaccessible places because the solar energy resource is the most geographically accessible in the globe. Power converter topologies and their control mechanisms play a major role in the performance of standalone PV systems [1]. To move electricity from DC PV modules to AC loads, two-stage power conversion is typically used [2], [3], [4], [5].The power DC-AC inverter is used in the second conversion stage to convert from DC to AC and to manage the load voltage or load current while the power converter is used in the first stage to increase the DC voltage and extract the most power possible from the PV modules [6], [7], [8], [9]. The Z-source inverter (ZSI) topology, on the other hand, is suggested as an alternative power converter design for photovoltaic systems [10], [11], [12], [13]. With fewer power electronics switches, the ZSI may perform the duties of a two-stage conversion system in a one-stage system [14],[15].The standalone power supply system's unbalanced loads can lead to harmonic distortion and unbalance in the load voltage [8],[16]. To address this problem, the Z-source four-leg inverter (ZSFLI) topology has been suggested. When there is an unbalanced load, ZSFLI offers a neutral wire to circulate the unbalanced current [17]. In spite of load unbalancing challenges, the ZSFLI can regulate the load current or voltage with proper control and good power quality.

In the standalone power supply system, the control of the power converter is crucial [18], [19], [20]. Numerous control strategies for the ZSI and the four-leg inverter have been put forth in the literature. Due to its capabilities, Finite Control Set Model Predictive Control (FSMPC) has recently attracted a lot of attention in the power electronics industry. Without employing the modulation stage, the FSMPC has directly controlled the converter switches. Additionally, the FSMPC has a quick transient response and its algorithm is simple, intuitive, and easily adaptable to the control objective [8], [9].

The standalone electrical system load current and ZS network capacitor voltage can both be controlled with high performance and quality using the FSMPC technique for ZSFLI that is presented in this thesis. In order to accomplish this, a precise discrete-time model of the standalone electrical system is developed, which enables the FSMPC to accurately forecast and control its controllable signal. The introduction of simulation results demonstrates the viability of the suggested method. The four chapters of this thesis are as follows:

The first chapter presents a basic description of microgrid structures in terms of electricity transmission and distribution, as well as the different structures of power converters used in standalone PV systems. Finally, it reviews the different topologies and controls for three-phase inverters.

The second chapter discusses photovoltaic systems, conventional inverters and Z- source inverters. It also introduces the characteristics, modeling of solar cells and modeling of Z- source inverters.

The third chapter describes the FSMPC (Finite Control Set Model Predictive Control) control technique for the four-leg Z-source inverter, which controls the voltage of the ZS network capacitor as well as the charging current of the electrical

system with high performance and quality. The effectiveness of the proposed technique is confirmed by the results of the simulation.

The fourth chapter presents the results of the simulations. These results validate the achievement of the research objective set in this work.

Chapter One: Theoretical Background study

1.1. Introduction

In the coming years, the notion of combining distributed energy resources for the formation of microgrids will be extremely important. A basic description of microgrid structures in terms of electricity transmission and distribution inside a microgrid opens this chapter. Next, we introduce a number of power electronics structures.Finally, we will go over the different topologies and controls for three phase inverters.

1.2. Renewable energy resources for power generations and microgrids

Fossil fuels are currently the world's main source of energy. However, the world is taking into account alternate energy generation methods that are more affordable and environmentally friendly [21]. The gradual depletion of fossil fuels and rising demand for electricity in both developed and developing nations are contributing factors, as are the high cost of expanding current centralized power generation plants, particularly in developing nations, the high cost of fuel in many remote areas, and concerns about greenhouse gas emissions and climate change. Future power production systems will incorporate renewable energy sources (RESs), such as wind turbines, photovoltaic solar systems, solar-thermal power, fuel cells, hydropower turbines, power micro-turbines, and hybrid power systems [22]–[24].

One of the promising solutions to the aforementioned technological and environmental issues is the usage of distributed energy resources (DERs) within microgrids. A microgridis described as a collection of distributed generation (DG) units, loads, power electronics, and energy storage systems that act as one unit under control [25]. Microgrids are being created in order to successfully promote the use of DERs and increase energy efficiency, power quality, transmission losses,

and consumer costs [26].Grid-connected microgrids and standalone microgrids are two different types of microgrids [27]. The grid-connected microgrid has two operational modes: grid-connected and islanding. When the microgrid is connected to the grid, the main control issue is efficient operation. When the microgrid disconnects from the utility due to abnormal circumstances, the main control issue is voltage and frequency control. Because freestanding microgrids are typically constructed in isolated locations, such as mountainous regions or islands without a power supply, they always operate in the islanding mode without being connected to the grid.

The method that microgrids transmit and distribute power can be used to categorize different microgrid configurations [4]. This category includes hybrid DC- and AC-coupled microgrids, AC microgrids, and DC microgrids.

1.2.1. DC Microgrids

DC distributed power systems are frequently used in electric vehicles, telecommunications systems, and other areas. Additionally, the widespread usage of electronic loads in commercial buildings and office buildings, along with the rapid expansion of photovoltaic (PV) and fuel cell systems, have elevated low-voltage direct current (LVDC) microgrid to the status of a desirable network solution. A typical LVDC microgrid structure is shown in Fig. 1.1, which is based on power electronics.

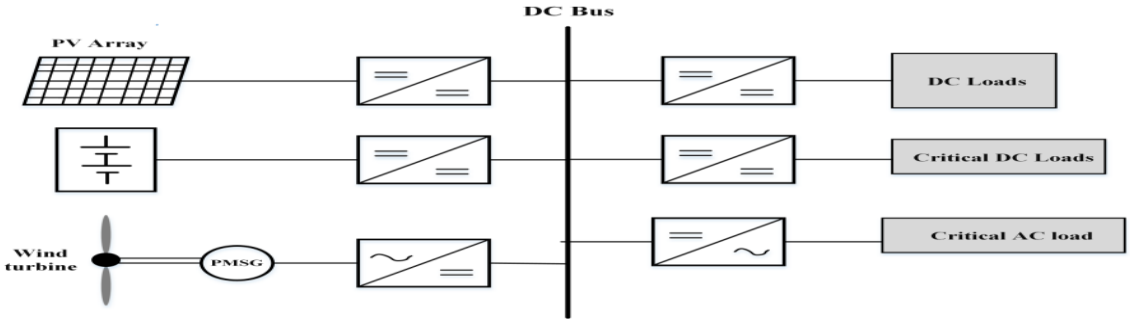

Fig. 1.1. Structure of DC microgrid

1.2.2. AC Microgrids

Since the microgrid concept was first put forth, AC microgrids have been the primary research focus. A common setup for power electronics-based AC microgridsis shown in Fig. 1.2.In this configuration, DERs are directly connected to the AC bus line and loads or utility through individual DC–AC or AC-AC converters [28], in one stage or two stages as will be discussed in the literature. The Microgrid can still provide the necessary quantity of electricity from the other sources even if one of the converters malfunctions [29]. To regulate the power and current pumped into the AC bus and/or utility, this system must use converters that need complex control algorithms and high-cost investments.

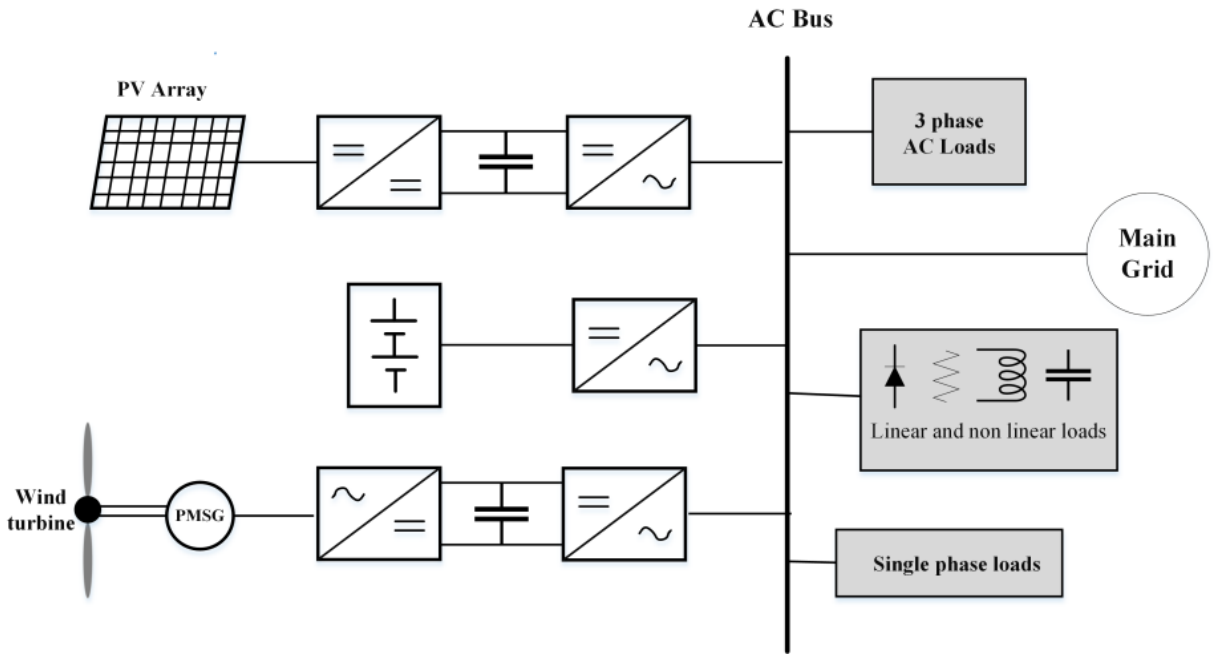

Fig. 1.2. Structure of AC microgrid

1.2.3. Hybrid DC- and AC-Coupled Microgrids

In [30], [31], hybrid DC- and AC-linked microgrids were introduced. It seeks to offer a practical method of incorporating various DER units into the current distribution system. The DC portion of hybrid DC- and AC-coupled microgridsis used to connect distributed energy storage systems, such as batteries, fuel cells, and even flywheels connected to bidirectional AC-DC converters, as well as other DC energy sources, such as PV systems connected through DC-DC Boost converters and small turbines (gas and wind) connected through rectifiers.To provide DC loads and maintain a consistent DC voltage at the input terminal of the DC-AC converter, the common DC bus gathers the regulated power from several DERs. The AC bus is connected to the common DC bus using a DC-AC inverter. The AC bus, which is flexible enough to integrate with the utility as depicted in Fig. 1.3, feeds the inverted power to the AC loads.

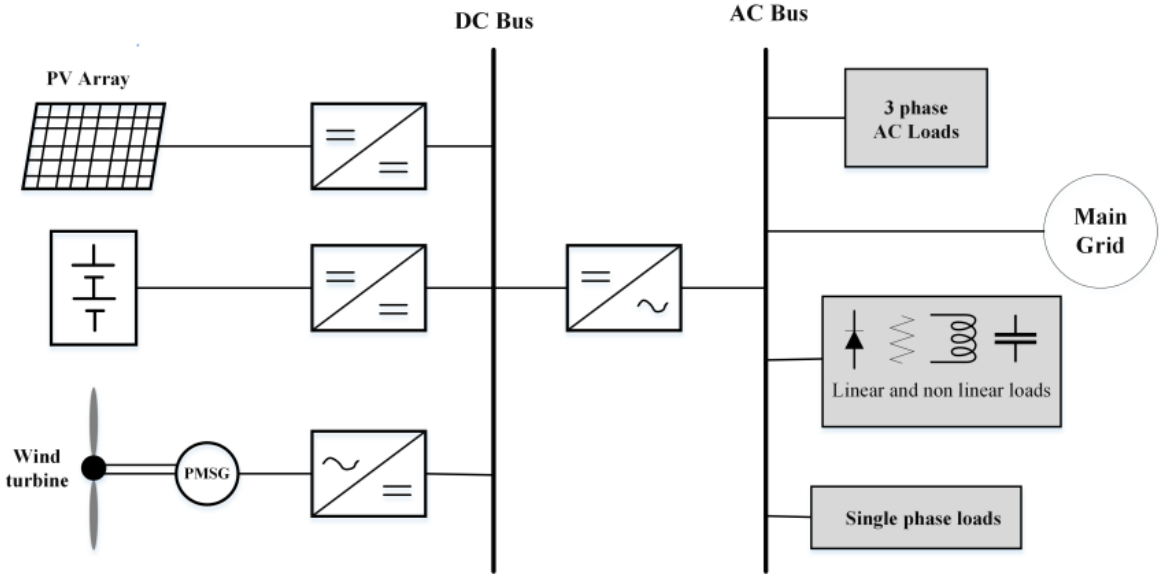

Fig. 1.3. Structure of Hybrid AC and DC linked microgrid

1.3. Structures of electronically-coupled DER units

The interface characteristics of DER units inside a microgrid can be used to differentiate between traditional rotating DG units and electronically-coupled DER units [32]. Through rotating generators, such as fixed-speed wind turbines, reciprocating machines, and small hydro turbines, the typical rotary DG units connect to the microgrid. The features of electronically-coupled DER units and the demands of grid circumstances are matched using power electronics converters. The electronically-coupled DER units include microturbines, RES-based DG units, and variable-speed wind turbines. The types of primary energy sources, load requirements, microgrid topologies, and related operational situations all affect how electronically-coupled DER units are built [33]. Accordingly, from the perspective of system structure, power converter topologies for DER units can be divided into two groups based on the quantity of power processing steps.

1.3.1. Two-Stage Power Conversion Systems

For all electronically-coupled DER units, the two-stage power conversion system is the most prevalent setup. Two typical two-stage power conversion system structures are shown in Fig. 1.4, one for a PV system and the other for a wind turbine system. A two-stage power conversion system typically consists of a grid-connected DC-AC converter and either an AC-DC converter or a DC-DC converter for energy sources with AC output voltage and DC output voltage, respectively. This configuration has two independent control systems; the first stage's control is for maximizing the amount of power from the input source, and the second stage's control is for managing the DC-link voltage as well as the output voltage and frequency.

1.3.2. Single-Stage Power Conversion Systems:

The fundamental design of a single-stage power conversion system for DER units that generate DC voltages is shown in Fig. 1.5. The advantages of this arrangement include great efficiency, small size and weight, and lower cost. Nevertheless, it requires a sophisticated control system to carry out the two stage configuration's purpose.

1.4. Inverter topologies

Two widely used inverter topologies are examined in this thesis, with each type subdivided into a number of subcategories.

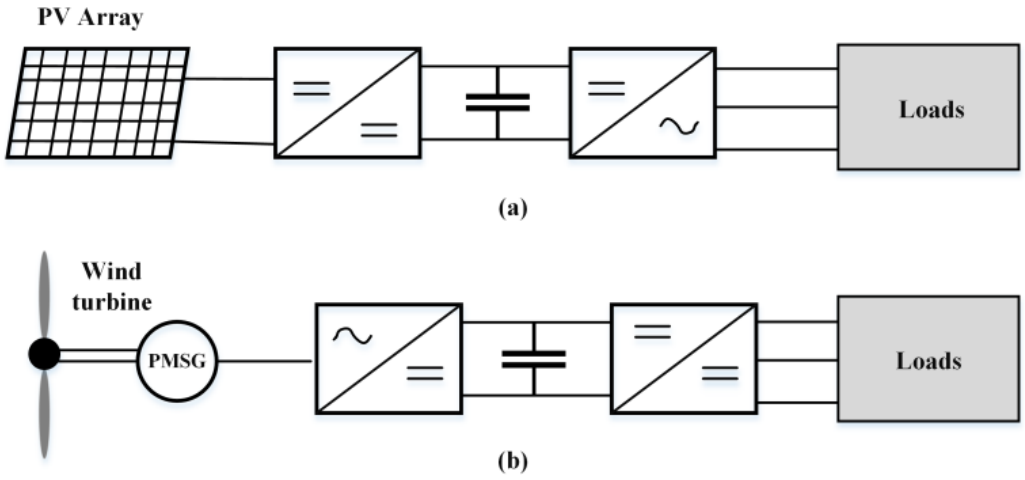

Fig. 1.4. Two structures of two-stage conversion systems. (a) for PV system. (b) for variable speed wind turbine system.

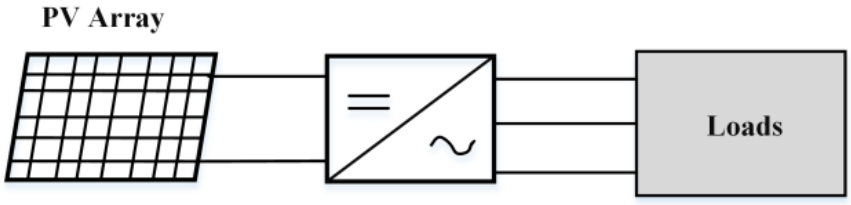

Fig. 1.5. The PV system's single-stage power conversion architecture.

1.4.1. Three-phase three-wire inverter topology

A three-phase, three-wire VSI structure is shown in Fig. 1.6. This topology is less interesting for a low-voltage distribution network, which is typically a four-wire system [34], as a neutral connection is needed to allow the circulation of zero sequence current components. However, the voltage unbalances and harmonics compensation ability can be achieved by proper control of the three leg VSI. An alternative is to utilize a three-leg inverter with a D-Y or zigzag transformer, although these are bulky, expensive, and unpopular in many applications [35–38].According to Figures 1.7 and 1.8, the zero sequence current component would be filtered in zigzag transformers or circulated in the D winding of D-Y transformers, leaving the control circuit of the inverter to only account for voltage drops caused by the positive and negative sequence currents on the inverter's output filter in the transformer's primary.

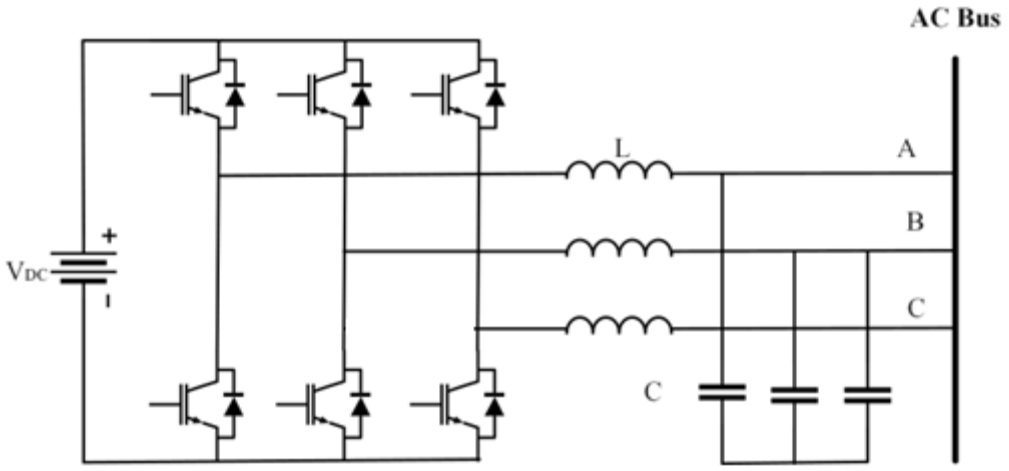

Fig. 1.6. Three-phase three-wire VSI topology

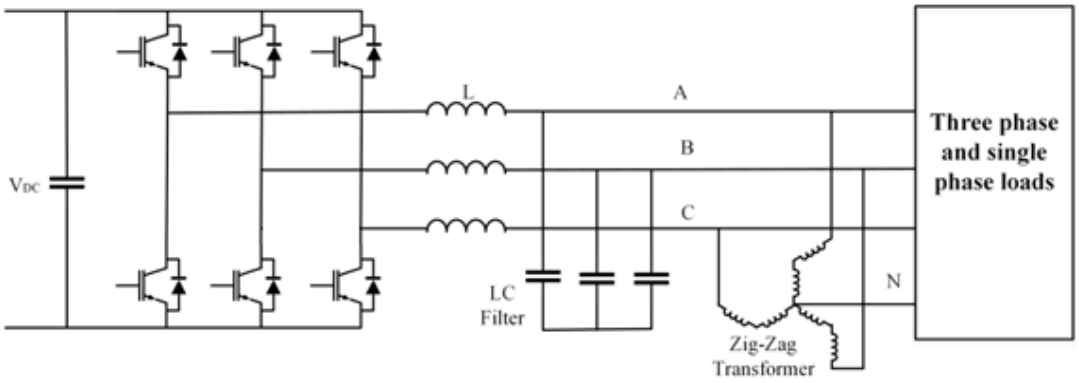

Fig. 1.7. Three-leg inverter with a Zig-Zag transformer

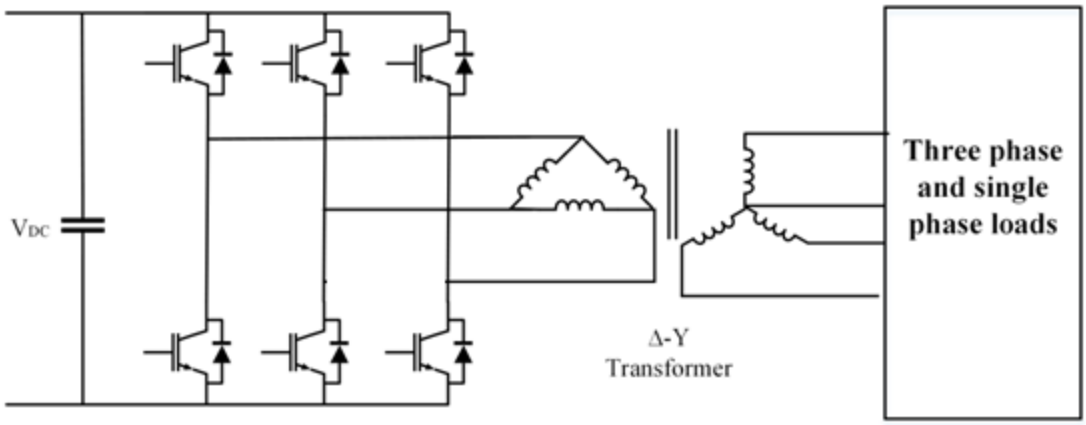

Fig. 1.8. Three-leg inverter with a D-Y transformer

1.4.2. Three-phase four-wire inverter topology

The advantages and disadvantages of the five primary methods of establishing a neutral connection for three-phase VSIs in three-phase four-wire systems are briefly described in this section [39],[40].

a. Capacitor midpoint topology

The simplest topology with the lowest switches is the capacitor midpoint topology, which is depicted in Fig. 1.9. The split dc-link capacitors' midway serves as the neutral in this design. Another benefit is that a three-phase split-link inverter may be controlled more easily than a four-leg inverter due to the fact that it essentially transforms into three single-phase half-bridge inverters and allows for independent control of each of the three legs [41]. To accomplish equal voltage sharing between the split capacitors, however, a costly and substantial capacitor is required [42]. Another drawback of this setup is that it can produce a disruption in the control strategy when subjected to extremely unbalanced and nonlinear situations by allowing a significant neutral current to pass through the neutral circuit.

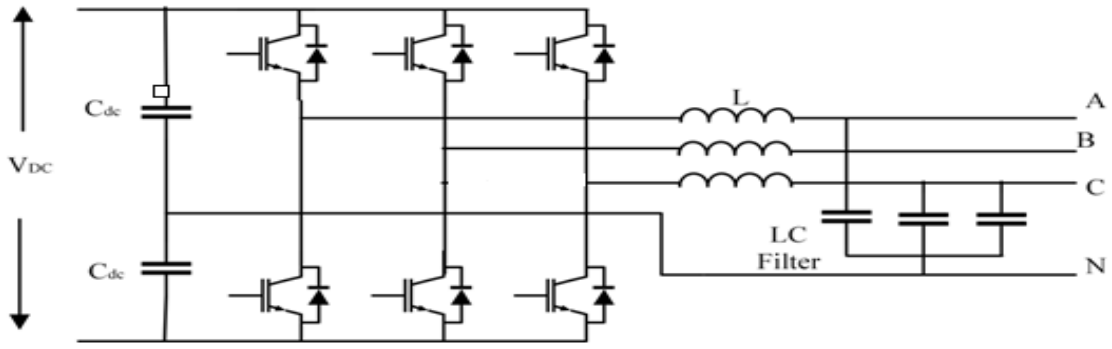

Fig. 1.9. Capacitor midpoint topology

b. Four-leg Voltage Source Inverter topology

Due to its effectiveness in managing unbalanced loads in four-wire systems, three-phase four-leg inverters are becoming more and more popular [43]. As shown in Fig. 1.10, the neutral point in this topology is created by joining the neutral path to the middle of the additional fourth leg. Large, expensive capacitors are not necessary in this design, which also offers slower DC-link voltage ripple. Additionally, compared to the split DC-link, the AC voltage in this setup may be

around 15% greater [22]. The topology becomes less interesting due to the additional two switches' difficult control. Nevertheless, four-leg inverters for three-phase four-wire applications are gaining popularity [44].

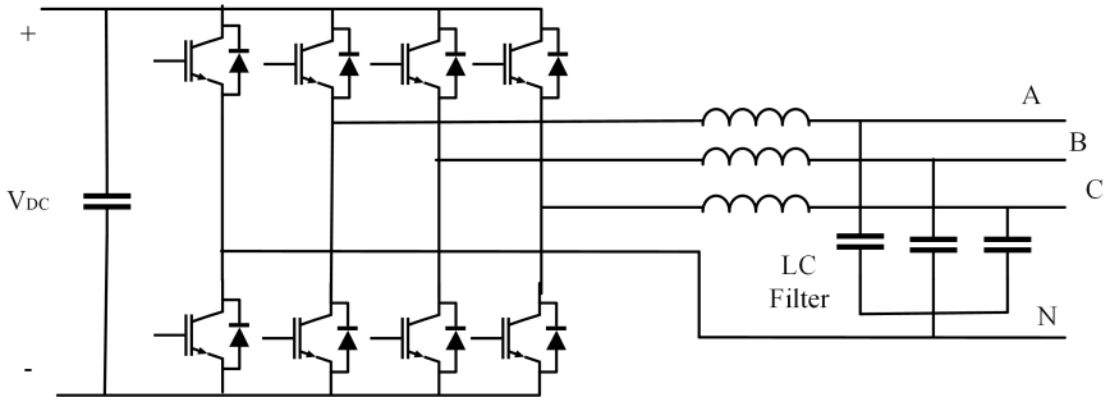

Fig. 1.10. Four-leg inverter topology.

c. Three H-Bridge Inverter

As shown in Fig. 1.11, this kind of power converter has three single-phase H-bridges to interface with the various output phases, each of which is connected to the utility grid by an isolation transformer. Four-wire active power filtering has been proposed using this architecture [45], [46]. This architecture has advantages over other topologies, such as a lower dc-link voltage required for a given output voltage that is half that of a capacitor midpoint inverter. Even though this power converter has a greater number of components, the output voltage it produces is identical to that of a three-level inverter, giving it a better harmonic profile and reducing the need for passive filters. Since each phase is independent from the others and the other two phases may continue source electricity to the grid in the event of a fault in any one phase, higher reliability can be attained. The main drawback of this topology is the demand for isolation transformer(s), which may not be a problem if isolation is necessary for safety and to comply with regulations.

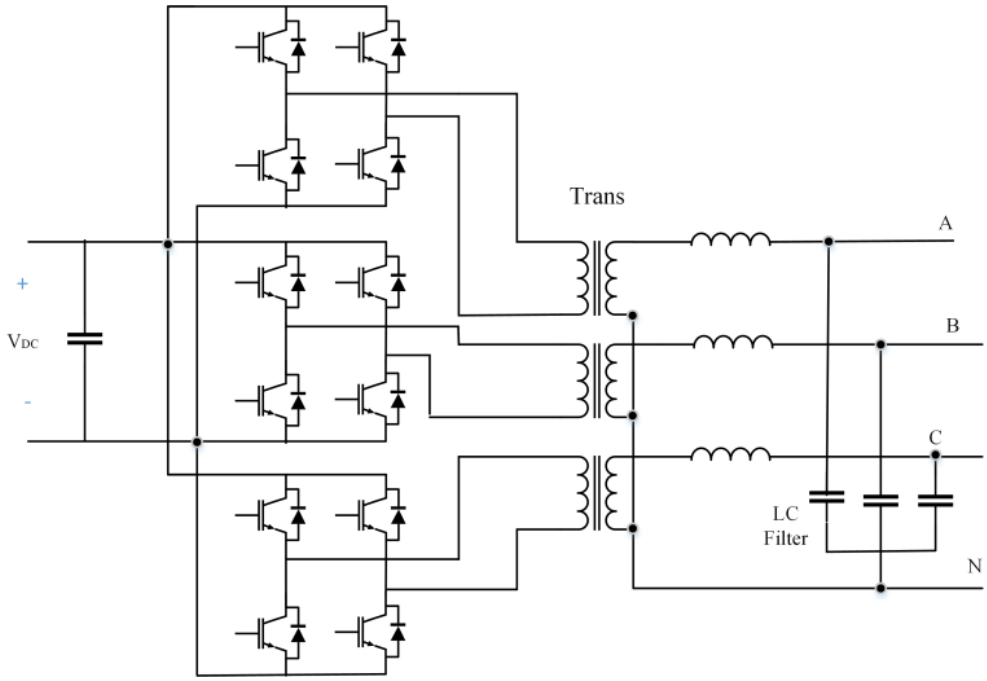

Fig. 1.11.Three H-bridge three-phase four-wire inverter.

d. Four leg impedance source inverters (ZSI)

There are some restrictions and issues with the voltage-source inverters (VSIs). The input voltage of VSIs must be higher than the line-to-line output voltage's peak value. In order to boost a low-voltage dc source to a desired ac output voltage, a dc-dc boost converter is therefore required as an input stage in applications with restricted accessible dc voltage, such as grid-connected photovoltaic (PV) generation and fuel cell power conversion [47]. Dead time is also necessary to prevent waveform distortion caused by the shoot-through of the upper and lower switching devices of each phase leg.

Z-source inverters (ZSIs) [48] have recently been proposed as a solution to these issues. With the right regulation, the ZSI may increase voltage to a magnitude that may be greater than the available dc link voltage in these inverters, which replace the dc-dc input stage [49],[50]. Fig. 1.12 depicts the ZS four-leg inverter structure. In reaction to the so-called shoot-through zero state of the inverter switching cycle,

the ZS's L-C impedance network, which is what it is built of, might increase the dc voltage. Two semiconductor switches in the same leg are turned on simultaneously in the shoot-through zero state to short-circuit the dc link. The energy is transmitted from the capacitors to the inductors in the ZS network during this stage, which is used to increase the dc voltage.

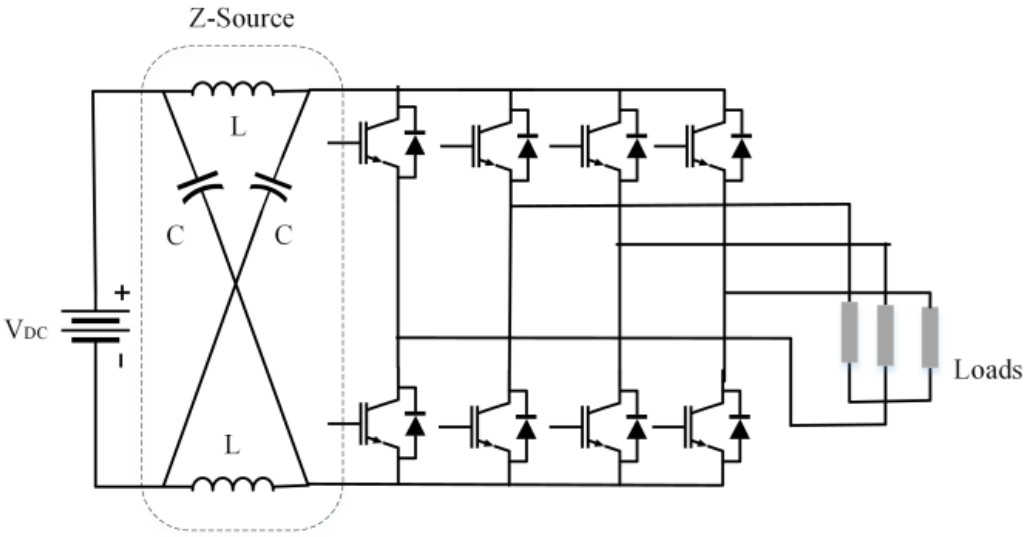

Fig. 1.12. Z-source three-phase four-leg inverter topology

Despite the benefits mentioned above, the main flaw in the Z-source inverter topology is that it is unable to control the inrush current and resonance that are introduced by the Z-source capacitors and inductors during startup, leading to a surge in voltage and current that could damage the devices [51]. It requires a more sophisticated control soft-start method to address this issue.

e) Four leg Matrix Converter (MC)

Power converter interfaces must be available to deliver constant frequency and voltage at the output when a variable speed generation system, such as a variable speed diesel-driven or wind turbine Permanent Magnet Synchronous Generator (PMSG), is utilized to supply electrical energy to isolated loads. To supply the neutral connection to the load in some applications, the generator is coupled to a

bridge rectifier and a 4-leg voltage source inverter (VSI) at the output [52][53].The 3-leg VSI can be used in place of the bridge rectifier to expand the operating speed range. In that situation, a back-to-back topology with seven legs—three at the generator-side converter and four at the load-side converter—requires two VSIs.

A 4-leg matrix converter (MC) can take the place of the 7-leg back-to-back converter [54]. This design offers sinusoidal input/output currents, variable input displacement factor, and bidirectional power flow [55]. The MC offers certain important advantages over back-to-back VSIs. For instance, the MC can be more durable and dependable without electrolytic capacitors. An MC has been able to conserve more room than a typical back-to-back converter [56] while still providing higher overall efficiency.But the matrix converter has also some disadvantages. It has a maximum output voltage that is restricted to about 87% of sinusoidal input waveforms, first of all. Additionally, it is extremely sensitive to changes in the input voltage system [55].

A 4-leg MC is shown coupled to a PM generator at the input in Fig. 1.1. At the output, the 4-leg MC is feeding a single load. The input current's total harmonic distortion (THD) is decreased by using a filter, which also provides the decoupling capacitors necessary for current commutation. The converter uses twelve bidirectional switches, each of which consists of two IGBTs and two diodes.

Table 1.1 presents a quantitative comparison of the four wire inverter topologies. Most experts agree that each topology has its own benefits and drawbacks and that only one topology can be applied to all applications.

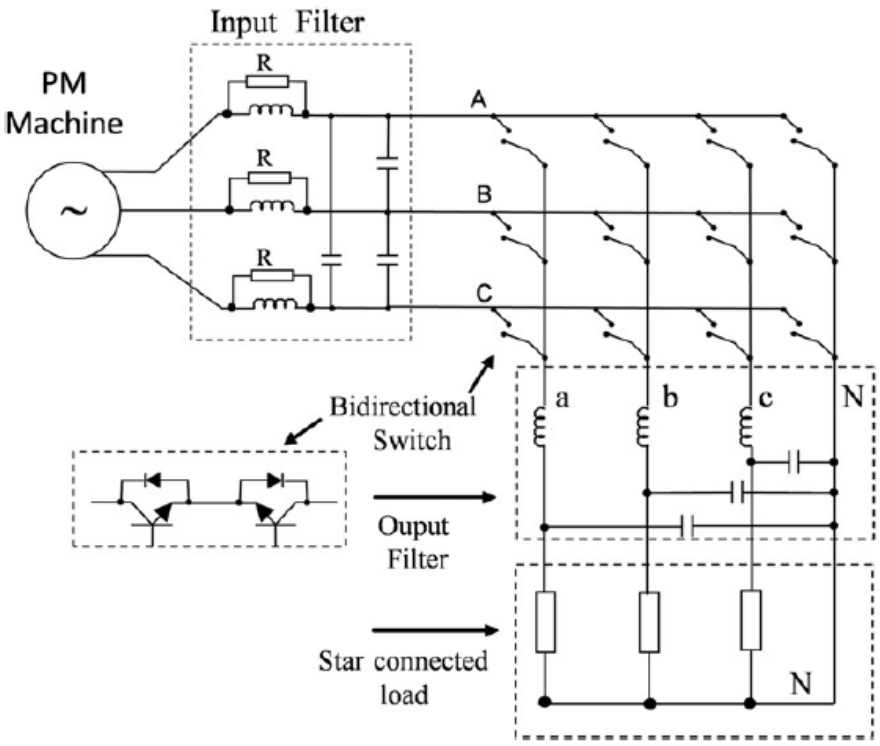

Fig. 1.13. A 4-leg matrix converter

Table 1.1. Comparison of Three-Phase Four-Wire Inverter Topologies

	Capacitor midpoint	**Four-leg VSI**	**3 H-Bridge Inverter**	**Four leg ZSI**	**Four leg MC**
Power conversion	DC-AC	DC-AC	DC-AC	DC-AC	AC-AC
Isolation transformer	no	no	yes	no	No
No. of switched	6	8	12	8	12 bidirectional
Input capacitor size	Very high	medium	low	high	No need
output voltage as a percentage of input voltage	<50% of input DC Voltage	<60% of input DC voltage	< 100% the input DC voltage	Can be grater or less than input DC Voltage	< 87 % of input AC voltage
Design complexity	low	high	medium	high	High
Size/wight	medium	low	high	medium	Low
Application in DG	Second stage converter for all types of DG	Second stage converter for all types of DG	Second stage converter for all types of DG	Single stage converter for PV and fuel cell DGs	Single stage converter for Variable speed diesel and wind DG

1.5. Control strategies for three phase inverters

The requirement for a given quality of the output voltage and current of the inverter dictates the need not only for the presence of an output filter, but also for appropriate control algorithms that allow maintaining the quality in dynamic modes with sudden changes in load. As a result, the generation unit must be covered by a feedback system, and the control system must have high performance in terms of processing input information and generating control signals for the inverters keys. The most popular control methods will be presented in this section [5].

1.5.1. PID control

The classic proportional-integral-derivative (PID) control has been the most commonly used method for many decades for a variety of applications. The advantage of this approach is its simplicity [57], [9]. The PID controller is used to control various systems DC under conditions. Therefore, the control of the system requires the Park transform to provide the system signals in dq0 reference frame from the abc natural reference frame. One of the disadvantages of PID control is that time and computational resources are spent on the processes of direct and inverse of Park transformation of the control signal. In addition, with mandatory measures to ensure the stability margin of the entire system, the formation of the differential component of the algorithm leads, as a rule, to an increase in noise. The control object is unstable because of the increased amplification of the high-frequency components of the error signal, which results in a decrease in the useful component of the control signal to noise ratio.

An important issue in the application of a PID controller is the process of adjusting its coefficients, which can be solved either on the basis of the experience of the designer, or on the basis of the use of automatic methods, for example,

Ziegler-Nichols or Rotach. Currently, there are several hundred methods of PID controller synthesis in the world, which are considered in particular in [58].

In technical systems, various forms of PID controllers are used, the number of which is more than ten [58]. The most famous and widespread form can be considered "classical", which has a transfer function of the form:

$$C(s)=k_p s+k_i/s + k_d s \quad (1.1)$$

1.5.2. Proportional resonant control (PR-control)

A frequency selective feedback channel tuned to the precise frequency of the output signal is a feature of proportional resonant control systems. Because there is no coupling between the control signals, PR-regulators can function in the natural coordinate system abc without the need for rotational transformations. Additionally, the PR controller is fairly resilient to changes in system settings [59], [60].Theoretically, the PR regulator forms a deep feedback with a large gain at the natural resonant frequency. So, the following is a representation of the PR controller's transfer function:

$$G_{PR}(S) = K_P + \frac{2K_i w_c S}{s^2+2w_c S+w_n^2} \quad (1.2)$$

Where n is the angular frequency of the output signal, c is the frequency of the resonance bandwidth, kp is the proportional gain, and ki is the integral gain of the resonant regulator.

The advantage of PR controllers is the ability to tune individual resonance in the frequency domain to accurately track and selectively compensate for unwanted harmonics. As shown in a number of works, the implementation of the PR controllers is not inferior in quality to the PI controller, but at the same time it requires lower computational costs. In three-phase systems, the PR controller has

the unique feature of both positive and negative sequence compensation. Also, the PR controller can be used directly in ABC coordinates [61].

1.5.3. H-Infinity control

A control designer depicts the control problem as an optimization problem, then solves it using H-infinity methods. Multivariable system issues are amenable to H-infinity approaches. However, it requires a good model of the system to be controlled and has a significant computational complexity. Furthermore, nonlinear restrictions are typically not handled well [62]. [63], [64], [65], [66] makes use of this controller.

1.5.4. Hysteresis control

Hysteresis control (HC) is an inverter control method in which the load current follows the reference current. This method has a non-linear control loop with hysteresis comparators. It operates with a variable switching frequency, which is considered a major disadvantage; the adaptive bandwidth of the controller must be designed in such a way as to limit the wide variation in the switching frequency. Variation in the switching frequency can cause a wide range of frequencies and high ripple currents, which make filter design difficult. Among the advantages of using hysteresis control are simplicity, reliability, independence of load parameters and good transient response.

1.5.5. Sliding Mode Control (SMC)

Pulse width modulation (PWM) inverters have been used with the sliding mode control (SMC) approach to control output voltage. The key benefits of this technique are its insensitivity to load disruptions and parameter changes. In the ideal scenario, invariant steady-state response can be attained. On the other hand, locating a suitable sliding surface is difficult. The efficiency of SMC will suffer at a low sample rate. Another downside of the SMC approach while following a

changeable reference is the chattering phenomena. As a result, the total system efficiency will suffer [67], [68], [69], [70], [71], [72].

1.5.6. Fuzzy control.

Fuzzy control is a technique for defining and applying a knowledgeable person's knowledge to control a system. The following parts make up this controller [73], [74], [75], [76], [77]:

• The rule-base is a set of guidelines for exercising control.

The inference mechanism uses information about the inputs formed by fuzzification and decides which rules are exerted on the current status; it also depends on what must be the plant input and forms conclusions. Fuzzification is the process of converting the numerical inputs into a form that can be used by the inference mechanism.

• Defuzzification converts the inference mechanism's conclusions into a numerical input for the plant. The fuzzy controller is employed here.

A system model is employed by the model predictive control (MPC) technique to forecast the future behavior of the regulated parameters. This is the output voltage (current) of the inverter in the context of a microgrid. Using this data and a predetermined objective function, the MPC determines the best course of control action. The process model blocks and the optimization module make up the predictive controller. A preliminary analysis of this method's applicability in the system design indicates that it has numerous benefits, including quick dynamic response, nonlinearity processing, and the capacity to incorporate restrictions in the control algorithm. The varied switching frequency of the keys is a drawback of the MPC implementation with variations in modes on the load side. The sample period, however, imposes a limit on the switching frequency. The microcontroller that uses

the MPC approach requires a lot more calculations than traditional controllers [78], [79], [16], [80].

1.6. Conclusion

The development of microgrids comes as a necessity for the integration of renewable energy sources into remote communities, and as an intermediate milestone towards the realization of the Smart Grid. This chapter provided an overview of microgrid. Following that, possible structures of electronically coupled DER units are described. Finally, the various inverter topologies and control methods of three phase inverters are presented.

Chapter two: Photovoltaic array and inverters

2.1. Introduction

The single stage inverter is a desirable choice because of qualities like dependability and affordability. However, its conventional design must be expanded to handle the significant photovoltaic (PV) voltage variance brought on by variations in temperature and irradiance. This chapter recommends utilizing a Z source inverter (ZSI) for solar system DC to AC power conversion.

2.2. Photovoltaic (PV) cells

PV cells are the fundamental building block of PV generators. The PV cells can be joined together to create PV modules, which are larger PV power generating units. PV arrays are constructed by joining several PV modules either in parallel or in series. PV generators can be created by electrically connecting the PV arrays. The basic unit, or PV cell, produces power in the range of 1 to 2 W [81]. However, they can also produce electricity in the MW range when combined with larger electrical units, such as PV arrays.

One of the simplest yet most accurate models of PV cells is the single-diode circuit. Other similar circuit models, such as the two-diode and three-diode models, take into consideration things like the impact of charge carrier recombination and significant leakage current on the photovoltaic cell, respectively. The single-diode equivalent circuit model of a PV cell is shown in Fig. 2.1, where $I_g$is a current source [A] connected in parallel with a diode and a parallel resistance R_p[Ω], $I_d$is the current flowing through the diode, $I_0$is the saturation current, and $R_s$is the series resistance. The thermal voltage of the module is given by the formula V_t=N_s *K* T/q ,where N(s) is the number of cells connected in series, T is the cell's

temperature, e=1.6*10(-19) [C], q is the electron charge, K is the Boltzmann constant, and I and V are the terminal current and voltage of the PV cell, respectively.

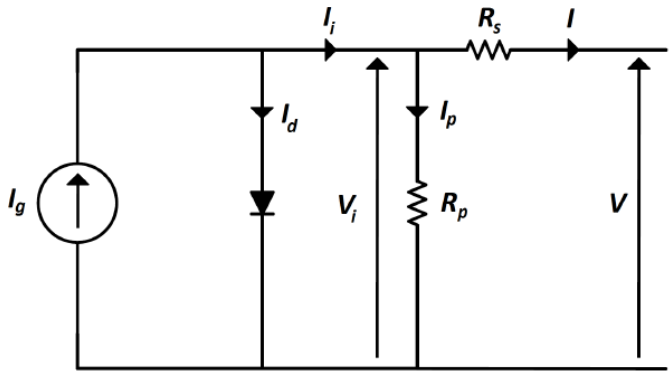

Fig. 2.1. Single-diode equivalent circuit of PV cell

By applying the Kirchhoff Rule:

$$I_g=I_d+I_p+I \tag{2.1}$$

The equation of the diode current:

$$I_d = I_0\ (exp(\frac{V+R_s.I}{v_t.a}) - 1 \tag{2.2}$$

The current is given in resistance Parallel:

$$I_p = \frac{V+R_s.I}{R_p} \tag{2.3}$$

From (2.1) we get current expression as:

$$I = I_g - I_d\text{-}I_p \tag{2.4}$$

The nonlinear equation describes how a PV Cell's characteristic (I-V) functions.

$$I = I_g - (I_0\ \left(exp\left(\frac{V+R_s.I}{v_t.a}\right) - 1\right))\text{-}\frac{V+R_s.I}{R_p} \tag{2.5}$$

2.3. PV array with conversional inverters

Traditional grid-tied PV systems typically employ a two-stage power conversion topology: a downstream dc/ac power conversion stage from the energy buffer to the grid, followed by an upstream DC-DC power conversion stage from the PV module to a dc link energy buffer (such as a capacitor). By producing ac voltages that are synched with the grid voltage and managing the operation's power factor, the downstream stage is in charge of regulating the flow of energy to the grid. Fig. 2.2 shows the main architecture of a traditional two-stage grid-tied PV system.

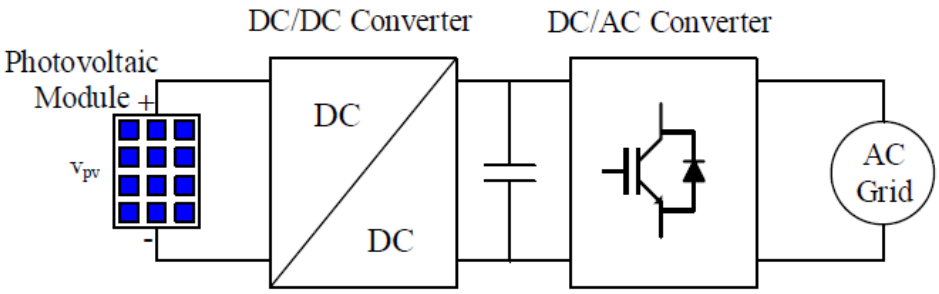

Fig. 2.2. Configuration of a two-stage grid-tied PV system

Due to the dc/ac inverters' intrinsic inability to step the voltage up or down freely, a two-stage design must be used. Commonly, voltage-source inverters (VSIs), also known as conventional inverters, can only step-down voltage, whereas current-source inverters (CSIs), also known as current-source inverters, can only step-up voltage (the VSIs can have a boost factor of almost 1.15, which is insufficient for most applications) [82], [83]. As a result, conventional dc/ac inverters often cannot freely step up and down the voltage.

2.3.1. DC-DC converters

Fig. 2.3 depicts a basic DC-DC boost converter device.

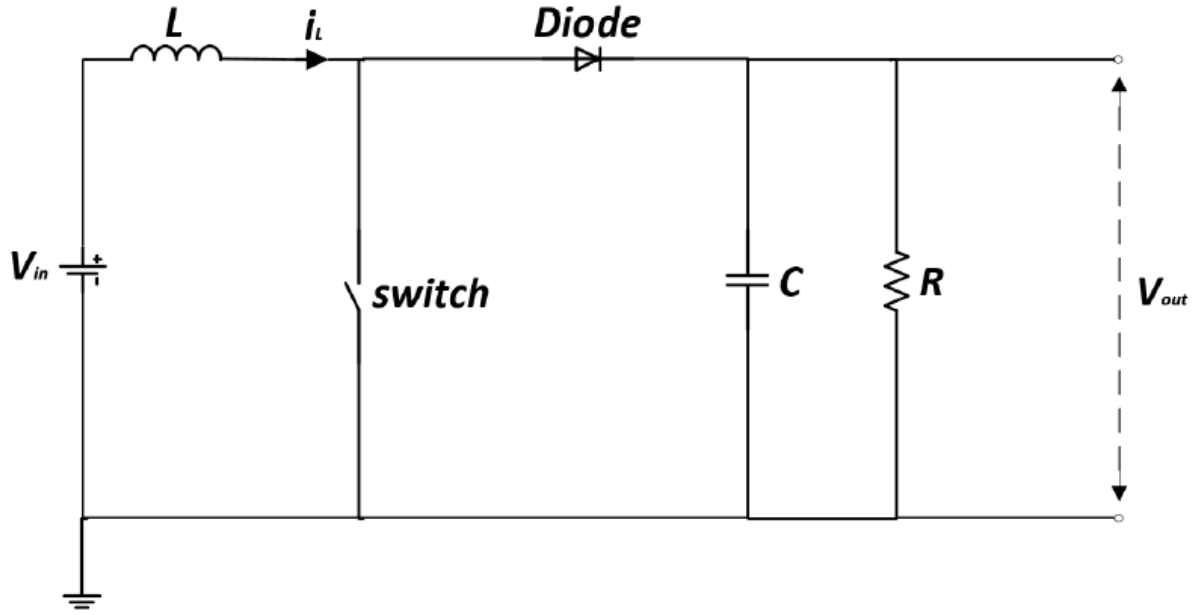

Fig. 2.3. Simple DC-DC boost converter circuit

Buck, boost, buck-boost, and flyback converters are the four main categories of DC-DC converters. Converters can be divided into isolated and non-isolated varieties.

Flyback converters are classified as isolated converters, whereas buck, boost, and buck-boost converters are classified as non-isolated converters. In contrast to non-isolated converters, which have no electrical isolation, isolated converters use a transformer for galvanic isolation. Other converters, such as the Cuk converter and the charge pump, are available in addition to the popular ones already listed. A non-isolated converter is the Cuk converter. Different DC-DC converters have the ability to change the output voltage that is supplied. A voltage step-up converter is a boost converter, and a voltage step-down converter is a buck converter. Since the power is constant, the current in the buck converter grows while it decreases in the boost converter. The output voltage can be stepped up or down using a buck-boost.

Buck-boost converters provide the same purpose as the flyback and Cuk. The transformer that separates input from output gives the flyback converter an isolating component. The applications range from LASERS and cell phone chargers to PC standby power sources. On the other hand, the charge pump converter is primarily utilized in low power applications. Additionally, it performs similarly to a buck-boost converter.

2.3.2. Inverters

Voltage source inverters (VSI) and current source inverters are the two broad categories into which the inverters can be divided (CSI). While the CSI is a voltage boost/step up inverter, the VSI is a voltage step down/buck inverter. Fig. 2.4 depicts the conventional voltage source inverter (VSI) system, while Fig. 2.5 depicts a current source inverter system.

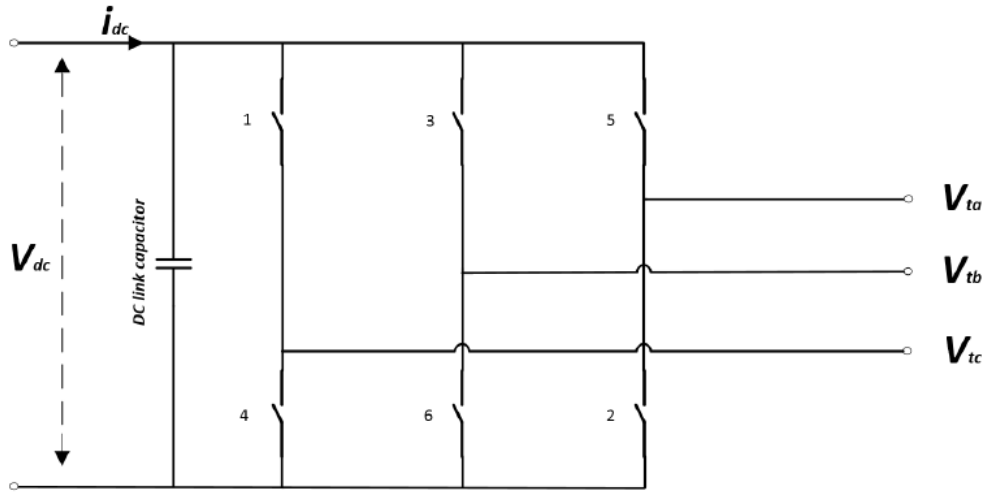

Fig. 2.4. a voltage source inverter system schematic diagram

The VSI has a voltage source and a large capacitor connected in parallel, whereas the CSI has a current source as its input. The output AC current is directly managed by the CSI. This means that although the CSI is a current stiff inverter, the VSI is a voltage stiff inverter. The use of VSI is found in electronic frequency changer circuits, ac motor adjustable speed drives, and uninterruptible power supply (UPS)

systems.

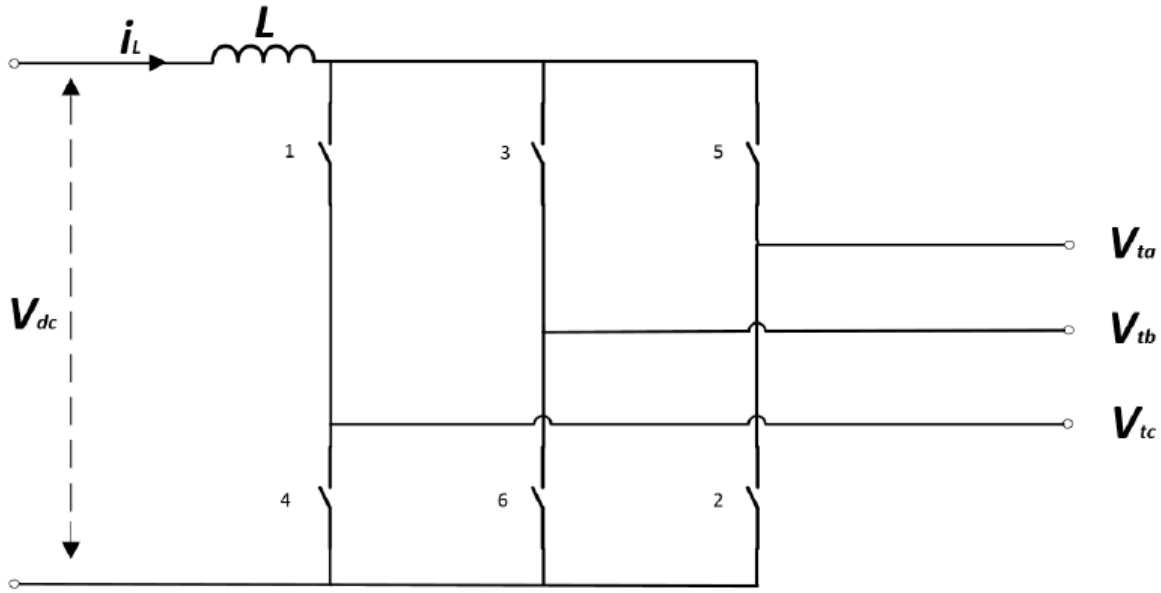

Fig. 2.5. An example of a current source inverter system's schematic

Despite being the more popular of the two types of inverters, the VSI has the following shortcomings and restrictions:

- Because the VSI is a voltage buck converter, it cannot be employed in situations when the input voltage is lower than the output voltage (required operation is buck). In order to achieve a voltage step-up for fuel cells and solar applications, a boost converter is utilized in addition to the VSI. Since another converter is also used, the cost goes up and the efficiency goes down.
- It is not possible to operate two phases simultaneously since doing so would result in the source shorting, also known as shoot-through, which would destroy the switches. As a result, a blanking period is added, which again results in higher harmonics.

In order to deliver a nearly sinusoidal voltage at the VSI output, a larger LC filter is required compared to CSI, resulting in power loss and poor efficiency.

Additionally, the I-source inverter (CSI) includes the following ceilings and restrictions:

- A voltage boost converter is the CSI. In order to step-down or boost the input voltage to the CSI, a buck/boost converter may be employed in some circumstances before the CSI. Since a second converter is also used, the price goes up and the effectiveness goes down (because there is another power conversion stage due to extra converter).
- The use of a series diode in tandem reduces the high performance of the IGBTs.

Additionally, the following issues are shared by VSI and CSI:

• Because of the range of output voltage that can be achieved, they can only be used in certain situations because they are either voltage buck or voltage boost inverters and not buck boost.

•The VSI and the CSI are both subject to electromagnetic interference (EMI) noise.

•They can not be substituted for one another because of the various sources required and output voltage ranges.

2.4. Z-source inverter (ZSI)

Despite being widely used in the industry, the VSI and CSI have limits because they can only function as voltage buck or voltage boost inverters, respectively [84]. In order to achieve the required output voltage, a boost converter must be connected before the VSI in the case of fuel cells or photovoltaic applications. In a

similar manner, a DC-DC converter must be connected before a CSI. Z-source inverters (ZSI) are preferable to them since it is a laborious operation to regulate two converters (the DC-DC converter and the inverter) along with an increase in prices. The ZSI is a single stage inverter that connects the DC source to the inverter via an X-shaped arrangement of capacitor and inductor. This enables operation in either the buck mode or the boost mode depending on the situation. Shoot through state is used in the unique network of two inductors and two capacitors to create buck and boost in the required configuration. The switches in the phase leg are concurrently shorted in the event of a shoot-through state. One phase leg at a time, two phase legs, or even all three could be used. Figure 2.6 depicts a ZSI's configuration.

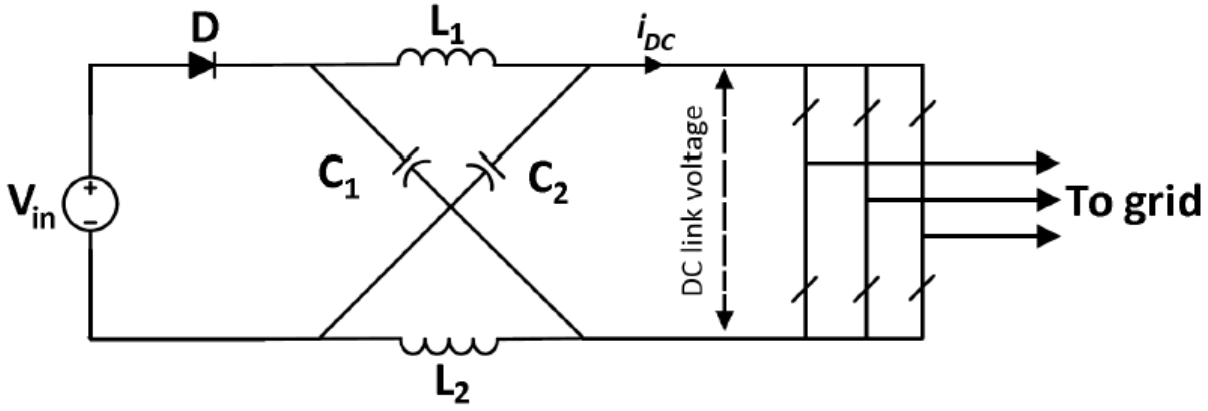

Fig. 2.6. Schematic diagram of a Z-source inverter system

Two inductors, L_1 and L_2, and two capacitors, C_1 and C_2, are connected in a crisscross X pattern to link the Z-source inverter to the DC voltage source, as shown in Fig. 2.6.

Since the output voltage of the cells is significantly variable depending on the exposure to light and the current drawn from the fuel stack, respectively, a boost converter is required when using photovoltaic and fuel cells as DC voltage sources. Since the VSI is a voltage buck converter, the boost converter ensures a voltage step-up. ZSI, on the other hand, is a single stage inverter that may, depending on the need, produce both the buck and boost of AC output. The ZSI features an additional zero state known as the shoot-through state in addition to the two zero states and six active states that are present in the VSI. A ZSI therefore has nine states altogether. If necessary, a voltage boost is made possible thanks to the shoot-through state. Additionally, it guarantees that blanking time, a standard characteristic of VSIs to prevent source short circuit, is not required.

The ordinary non-shoot-through mode and the shoot-through mode are the two operational modes for the ZSI. In the non shoot-through mode, are shown in Fig. 2.7(a) ,the ZSI operates like a VSI or CSI with the regular eight states (six active and the remaining two zero states), while the shoot-through mode, depicted in Fig. 2.7(b), involves the source being shorted across one or more phase legs, which is prohibited in a conventional inverter.

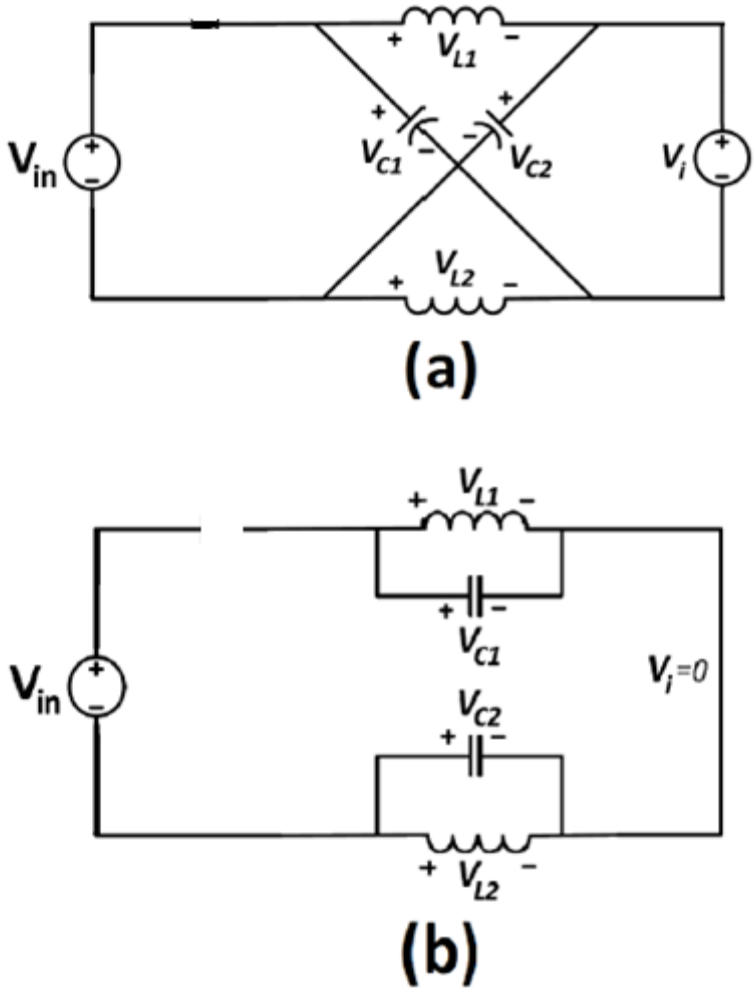

Fig. 2. 7. (a) ZSI's analogous circuit model with no shoot-through states. Model of the ZSI's shoot-through state equivalent circuit (b)

As components of the ZSI network are similar:

$$V_{c1} = V_{c2} = V_c \quad (2.6)$$

$$V_{L1} = V_{L2} = V_L \quad (2.7)$$

During T_0,when the inverter is working in the shoot through mode as shown in figure 2.7.b

$$V_L = V_C \quad (2.8)$$

$$V_i = 0 \quad (2.9)$$

$I_{in} = 0$ (2.10)

$$L * \frac{di_L}{dt} = V_c \quad (2.11)$$

$$C * \frac{dVc}{dt} = -i_L \quad (2.12)$$

For the period of T_1 as $T = T_1 + T_0$ while non-shoot through mode :

$V_L = V_{in} - V_c$ (2.13)

$I_{in} = i_L + i_c$ (2.14)

$$L * \frac{di_L}{dt} = V_{in} - V_c \quad (2.15)$$

$$C * \frac{dVc}{dt} = I_{in} - i_L \quad (2.16)$$

The boost factor is presented as :

$$B = \frac{T}{(T_1 - T_0)} \quad (2.17)$$

In the following equation the peak voltage of the output is given :

$$v_{ac(max)} = MB \frac{V_{in}}{2} \quad (2.18)$$

M : the modulation index[85]

The voltage through the capacitor is :

$$V_c = \frac{1-D}{1-2D} v_{in} \quad (2.19)$$

D : the shoot-through duty ratio

Lastly the voltage stress can be represented as:

$$v_i = B * V_{in} \quad (2.20)$$

The following are only a few of the advantages ZSI has over conventional VSI or CSI:

- A battery is not the only DC source of input; there are a wide variety of other sources as well, such as voltage or current sources or even loads like diode rectifiers, thyristor converters, inductors, capacitors, etc.
- There are a variety of uses for the ZSI, including variable output voltage sources like fuel cells and solar arrays. Thus, the AC voltage can be adjusted to any value between zero and extremely high magnitudes. VSI or CSI do not possess the buck-boost inverter that the ZSI possesses.
- Some PWM scheme can be used to control the ZSI. Consequently, it also provides a lot of freedom.
  • It is applicable to all power conversion ranges [48].

2.5. Conclusion

The Z-source inverter overcomes the conceptual and theoretical barriers and limitations of the traditional voltage-source inverter and current-source inverter and provides a novel power conversion concept. In this chapter we presented the photovoltaic system with conventional inverters. Next we proposed other inverter which is Z-source inverter because it is fulfills buck-boost capability in single stage topology.

Chapter Three: Control of Z -source inverter

3.1. Introduction

This chapter describes the Finite Control Set Model Predictive Control (FSMPC) technique for the Z-source Four Leg Inverter (ZSFLI), which controls the ZS network capacitor voltage as well as the load current of the standalone electrical system with high performance and quality. In order to accomplish this, a precise discrete-time model of the standalone electrical system is developed, which enables the FSMPC to accurately forecast and control its controllable signal. The efficiency of the suggested technique is confirmed by the simulation results.

3.2. The standalone of electrical system with Z- source four leg inverter

Power converter topologies and their control mechanisms play a major role in the performance of standalone electrical systems [1]. To move electricity from DC electrical modules to AC loads, two-stage power conversion is typically used [2], [86], [4], [5]. The power DC-AC inverter is used in the second conversion stage to convert from DC to AC and to manage the load voltage or load current while the power converter is used in the first stage to increase the DC voltage and extract the most power possible from the electrical systems modules [6], [7].The Z-source inverter (ZSI) topology, on the other hand, is suggested as a different power converter design for electrical systems [10], [11], [12], [13]. With fewer power electronics switches, the ZSI may perform the duties of a two-stage conversion system in a one-stage system [14], [15]. The standalone power supply system's unbalanced loads can lead to harmonic distortion and unbalance in the load voltage [8], [16]. To address this problem, the Z-source four-leg inverter (ZSFLI) topology has been suggested. Under unbalanced load conditions,

ZSFLI has a neutral wire for recirculating the unbalanced current [17]. In spite of load unbalancing challenges, the ZSFLI can regulate the load current or voltage with proper control and good power quality. In the standalone power supply system, the control of the power converter is crucial [18], [19], [20]. Numerous control strategies for the ZSI and the four-leg inverter have been put forth in the literature. Due to its capabilities, Finite Control Set Model Predictive Control (FSMPC) has recently attracted a lot of attention in the power electronics industry. Without employing the modulation stage, the FSMPC has directly controlled the converter switches. Additionally, the FSMPC offers a quick transient reaction and an easy algorithm that is simple to modify and tailor to the control target [8], [9].

3.3. Modeling of Z -source inverter

Figure 3.1 depicts the electrical system under investigation, which consists of a ZSFLI, an RL-filter, and a load. In place of the dc-dc converter in conventional two-stage power conversion, the ZSFLI has the ZS network. You could think the electrical system as the ideal source.

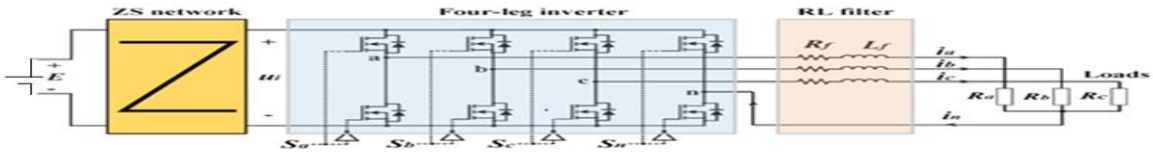

Fig. 3.1. Standalone electrical system with ZSFLI

3.3.1. Mathematical Model of ZS network

The non-shoot-through state and the shoot-through state are the two operational states of the ZS network [48]. Fig. 3.2 depicts the equivalent circuits of the ZS network along with its states. According to Fig. 3.2, the ZS network consists of two capacitors (C_1 andC_2) and two inductors (L_1 and L_2).

To make the ZS network symmetrical, it can be assumed that the two inductors have the same inductance and the two capacitors have the same capacitance:

$$\begin{cases} U_{C1} = U_{C2} = U_C \\ u_{L1} = u_{L2} = u_L \end{cases} \quad (3.1)$$

Two semiconductor switches in the same leg of the inverter are simultaneously closed in the shoot-through zero state for an interval (T_0), during the switching cycle (T), resulting in a short-circuit across the dc link. As seen in Fig. 3.2b, the inverter is modeled during this state as a short circuit for the ZS network. In this instance, the ZS network's energy is transferred from the capacitors to the inductors, increasing the dc voltage. Starting with the equivalent circuit, Fig.3.2b, the inductor voltage (u_L), diode voltage (u_d), DC-link voltage (u_i) are:

$$\begin{cases} u_L = U_C \\ u_d = 2U_C \\ u_i = 0 \end{cases} \quad (3.2)$$

Two semiconductor switches in the same leg of the inverter are not simultaneously closed in the non shoot-through zero state for an interval (T_1), during the switching cycle (T), As seen in Fig. 3.2c, the inverter is modeled during this state as a constant current source. Starting with the equivalent circuit:

$$\begin{cases} u_L = E - U_C \\ u_d = E \\ u_i = U_C - u_L = 2U_C - E \end{cases} \quad (3.3)$$

E is the DC voltage coming from electrical source. According to (3.2) and (3.3), the average inductor voltage over one switching period ($T = T_0+T_1$) across the inverter should be zero in steady state.

$$U_L = \frac{T_0 U_C + T_1 (E - U_C)}{T} \quad (3.4)$$

$$\frac{U_C}{E} = \frac{T_1}{T_1 - T_0} \tag{3.5}$$

Similar results can be obtained for the average dc-link voltage across the inverter bridge:

$$U_{i\_av} = \frac{T_0 \times 0 + T_1(2U_C - E)}{T} = \frac{T_1}{T_1 - T_0} E = U_C \tag{3.6}$$

As shown in (3.3), the peak dc-link voltage across the inverter bridge is expressed as:

$$U_{i\_peak} = U_C - u_L = 2U_C - E = \frac{T}{T_1 - T_0} E = BU_C \tag{3.7}$$

Where

$$B = \frac{T}{T_1 - T_0} = \frac{T}{1 - 2\frac{T_0}{T}} \geq 1 \quad , \tag{3.8}$$

is the boosting element brought on by the shoot-through zero condition.

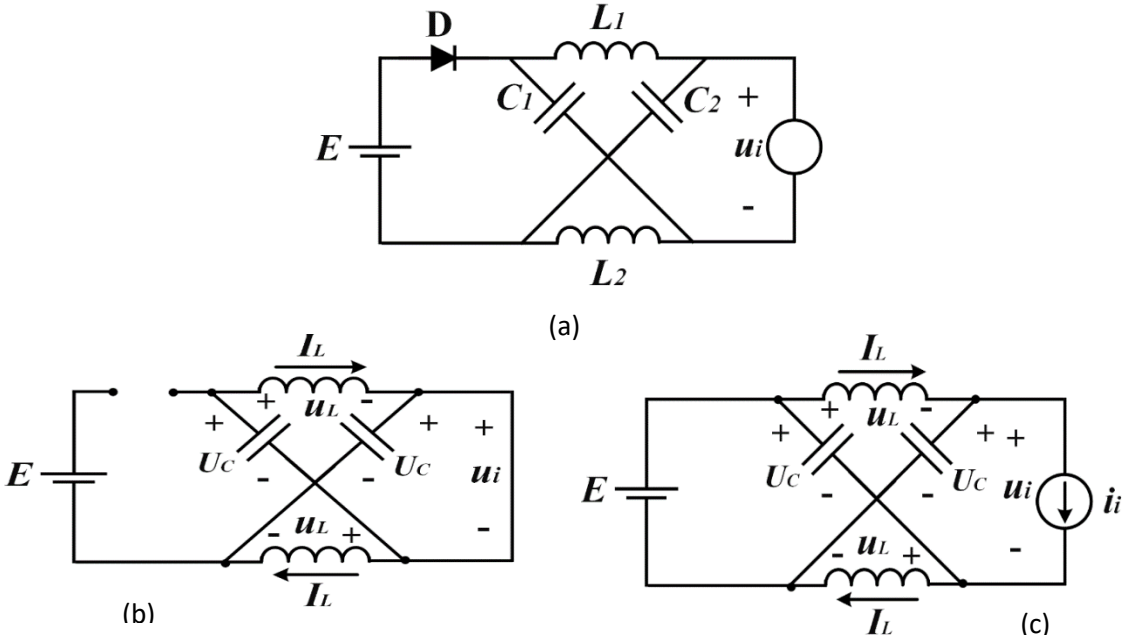

Fig. 3.2.(a) The Z-source inverter's equivalent circuit (b) in shoot-through zero states (c) in a state that isn't shoot-through. Mathematical model of the four-leg inverter

Fig. 3.1 depicts the four-leg inverter with the RL filter and loads. The following is an expression for the output inverter voltage:

$$\left.\begin{aligned} u_{an} &= (S_a - S_n)u_i \\ u_{bn} &= (S_b - S_n)u_i \\ u_{cn} &= (S_c - S_n)u_i \end{aligned}\right\} \tag{3.9}$$

By using the Kirchhoffs voltage law on the inverter's output circuit:

$$\left.\begin{aligned} u_{an} &= (R_{fa} + R_a)i_a + L_{fa}\frac{di_a}{dt} \\ u_{bn} &= (R_{fb} + R_b)i_b + L_{fb}\frac{di_b}{dt} \\ u_{cn} &= (R_{fc} + R_c)i_c + L_{fc}\frac{di_c}{dt} \end{aligned}\right\} \tag{3.10}$$

This equation can be expressed as follows:

$$u_j = (Rf_j + R_j)i_j + Lf_j\frac{di_j}{dt} \tag{3.11}$$

where j = a,b,c. Neutral current in can be expressed as:

$$i_n = i_a + i_b + i_c \tag{3.12}$$

3.4. Finite set Model predictive control

Fig. 3.3 shows the block diagram of the proposed FSMPC scheme for the FLZSI. Given that this control technique's algorithm utilizes the discrete model of the system and is repeated for a predetermined sampling period, it can be categorized as a digital control technique (T_s). For a one-step prediction horizon (k+1), where k is the sampling instant, the proposed FSMPC algorithm predicts the load current (ij), the voltage (U_c), and the current (I_L) of the ZS network using the discrete predictive model of the electrical system. This prediction is made for each FLZSI switching state. The best switching state is chosen using the objective

function in order to reduce the difference between the predicted current and voltage values and the reference values. The inverter switches are then subjected to the chosen switching state. Figure 3.4 shows the algorithm's flow diagram.

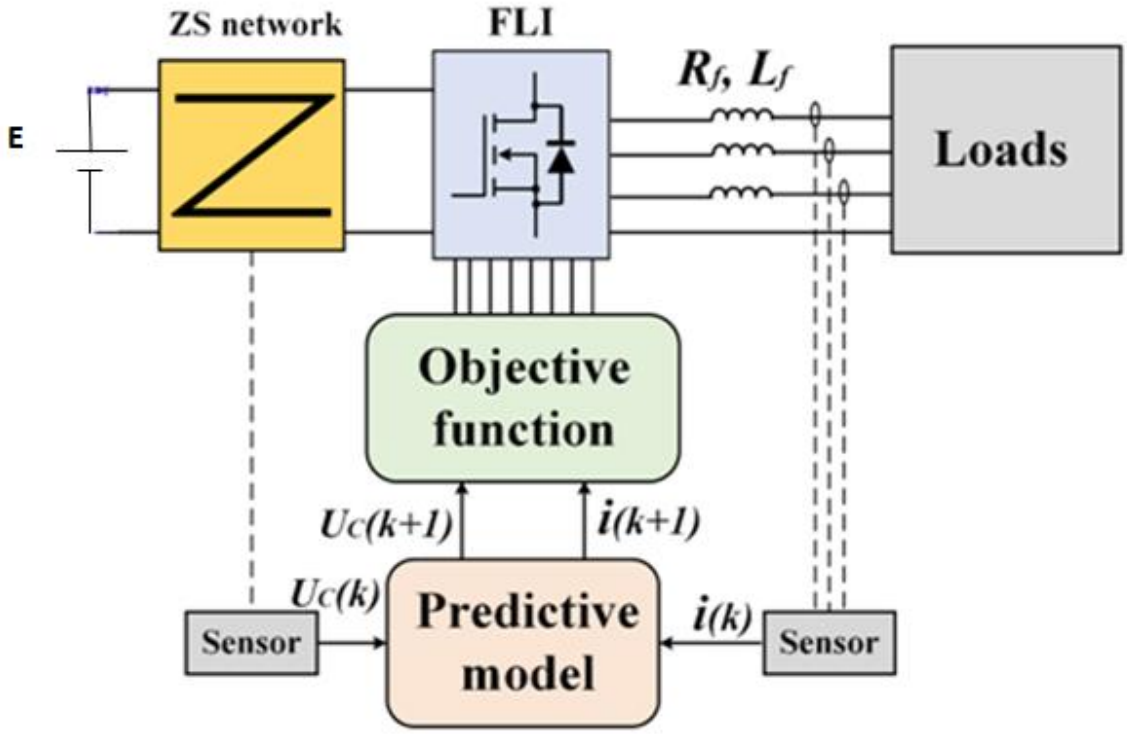

Fig. 3.3.The proposed FSMPC block diagram for the electrical system.

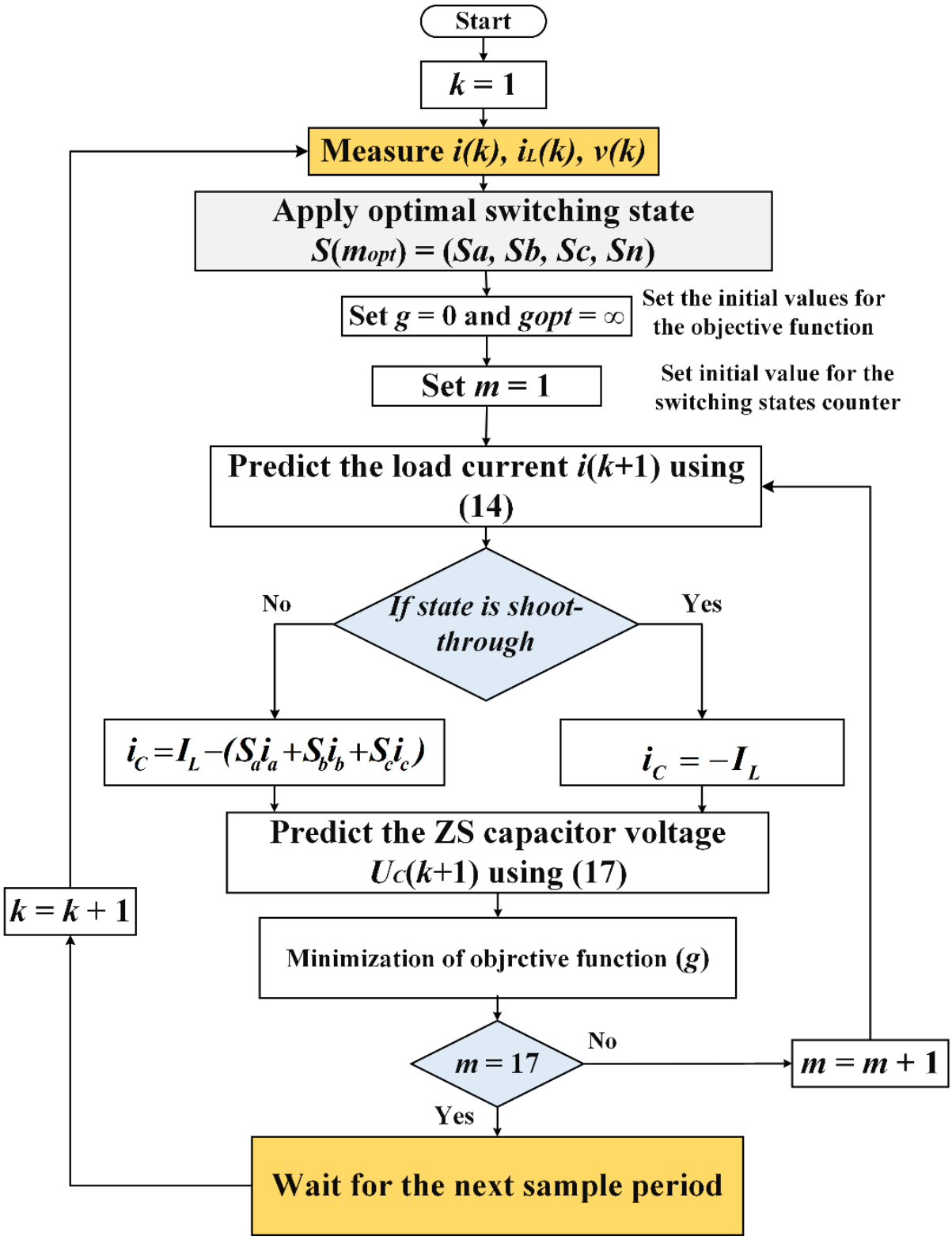

Fig. 3.4. Flowchart of the proposed FSMPC algorithm for FLZSI.

3.4.1. The system's predictive model

The two parts of the predictive model are as follows:

1) Part I of the predictive model

The load currents are predicted using this component. The derivative value of load currents can be expressed as follows from (3.11):

$$\frac{di_j}{dt} = \frac{1}{Lf_j}[u_j - (Rf_j + R_j)i_j] \tag{3.13}$$

The predicted load current for the following sampling instant (k+1) can be expressed as follows by applying the forward Euler rule [87]:

$$i_j(k+1) = \frac{Ts}{L_f + (R_j + R_{fj})Ts} u_j(k+1) + \frac{Ts}{L_f + (R_j + R_{fj})Ts} i_j(k) \tag{3.14}$$

2) Part II of the predictive model

This component forecasts the ZS network's capacitor voltage (U_c). The equivalent circuit of the ZS network is depicted in Fig. 3.2a, and it can be used to express the ZS capacitor current as follows:

$$i_C = C\frac{dU_C}{dt} \tag{3.15}$$

Where C is the ZS capacitor's capacitance. The capacitor voltage can be calculated as follows from (3.15):

$$\frac{dU_C}{dt} = \frac{1}{C} i_C \tag{3.16}$$

The predicted value of the capacitor voltage for the following sampling instant (k+1) can be calculated by applying the forward Euler rule as follows:

$$U_C(k+1) = U_C(k) + \frac{Ts}{L} i_C(k) \tag{3.17}$$

Where $i_C(k)$ is the ZS capacitor current for the current sampling instant (k), which depends on the non-shoot-through and shoot-through states of the ZSFLI topology:

a) For the state that isn't shoot-through:

$$i_C = I_L - (S_a i_a + S_b i_b + S_c i_c) \tag{3.18}$$

b) for the state of the shoot-through:

$$i_C = -I_L \tag{3.19}$$

3.4.2. Objective function

Three objective functions are combined into one multi-objective function in the proposed FSMPC. the other two objective functions, which are for the ZS inductor current and capacitor voltage, respectively, and one objective function for the load current. The following is an expression for the multi-objective function:

$$g = g_i + \lambda g_C \tag{3.20}$$

Where g_i is the load current's objective function and is denoted by:

$$g_i = [i_j^* - i_j(k+1)]^2 \tag{3.21}$$

Where j = a,b,c. i_j^* the standard load current. g_C is the ZS capacitor voltage's objective function, which is written as:

$$g_C = [U_C^* - U_C(k+1)]^2 \tag{3.23}$$

Where $U_C^*$is the reference voltage for the ZS capacitor. Utilizing the objective function classification technique described in [88], [89], the weighting factor (λ) was established.

3.4.3. The proposed FSMPC Algorithm

Fig. 3.4 provides the flowchart for the proposed FSMPC algorithm. The FSMPC algorithm can be summed up as follows:

- Check the ZS capacitor voltage, ZS inductor current, and load currents.
- For each switching state, predict the load currents, ZS inductor current, and ZS capacitor voltage using the predictive model.
- For each switching state, evaluate the objective function (g).
- Decide on the switching state that provides the objective function's minimum value (g).
- Put the ZSFLI switches in the switching state.

3.5. Conclusion

This chapter illustrates a model predictive control (MPC) system for a Z-source four leg inverter. The mathematical models of this inverter are provided. To control this inverter, a detailed finite set model predictive control has been described.

Chapter Four: Results and Discussion

4.1. Introduction

Simulation has been carried out using the configuration shown in Fig. 3.1 in Matlab/Simulink in order to validate the theoretical analysis and support the proposed FSMPC technique of ZSFLI. Table 4.1 provides the system parameters.

Table 4.1. System Parameters

Parameters	Values
DC input voltage of the inverter	V_{dc} = 150-250 V
Reference capacitor voltage	U_C = 635 V
ZS inductances	L_1=L_2=L = 1.5 mH
ZS capacitances	C_1=C_2=C= *470* µF
Load resistance	R = *5-25* Ω
Unbalanced nonlinear loads	L'_a=50mH,R'_a=20Ω,R_b1'=1Ω, R_b2'=60Ω, C'_b=3000µF,L'_c =20mH,R'_c=60Ω,C'_c=3000µF
Filter parameters	L_f = 10mH, R_f = 0.05 Ω
Nominal frequency	F = *50* Hz
Switching frequency	f_s=5000 Hz
Sampling time	T_s = 20 µs

4.1.1.Case1 :Loads Resistance (R)

1- Unbalanced Resistance R ($R_1 \neq R_2 \neq R_3$)

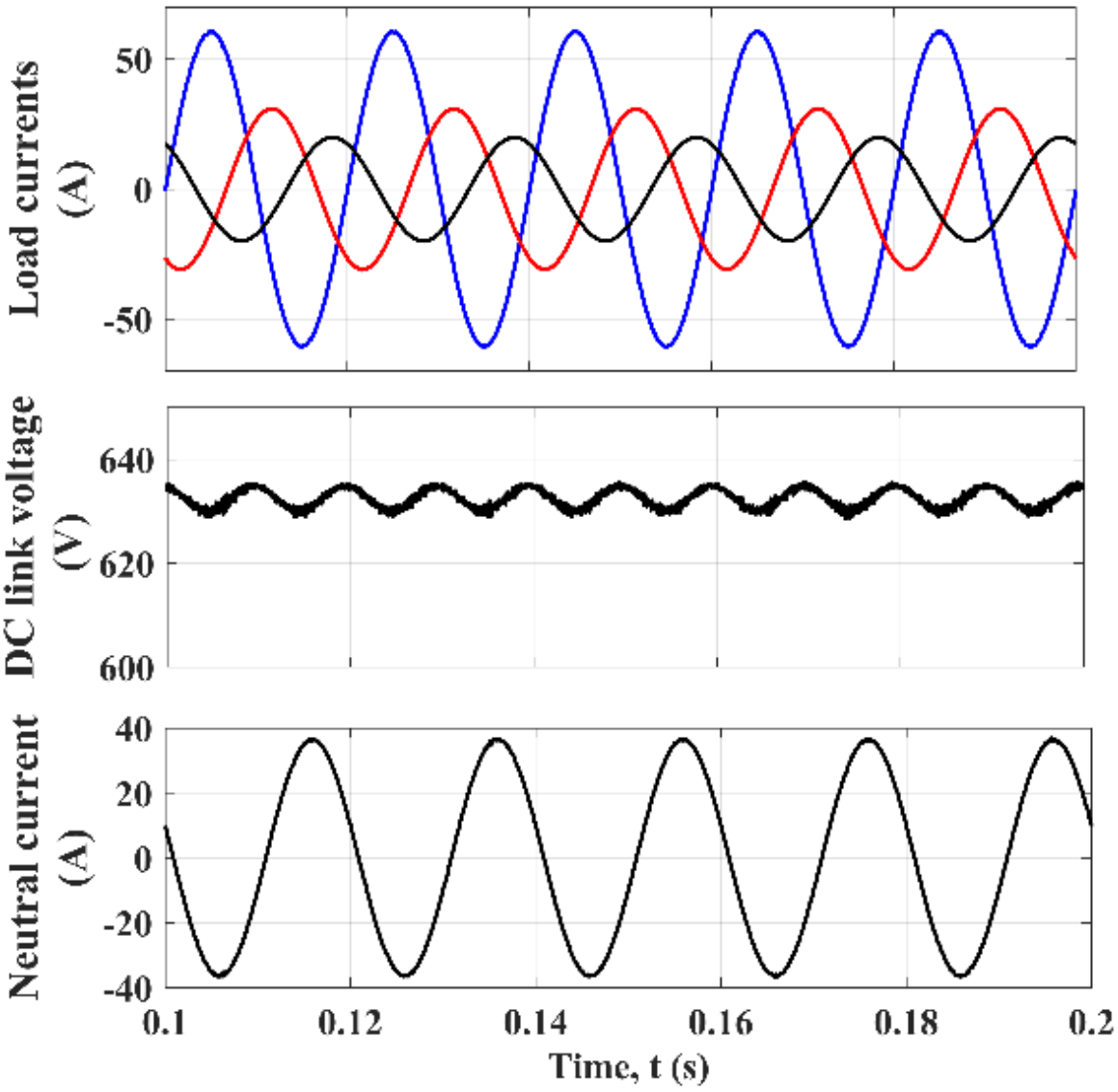

Fig. 4.1.A steady state is produced with unbalanced load current references.

2-Balanced Resistance R (R_1=R_2=R_3)

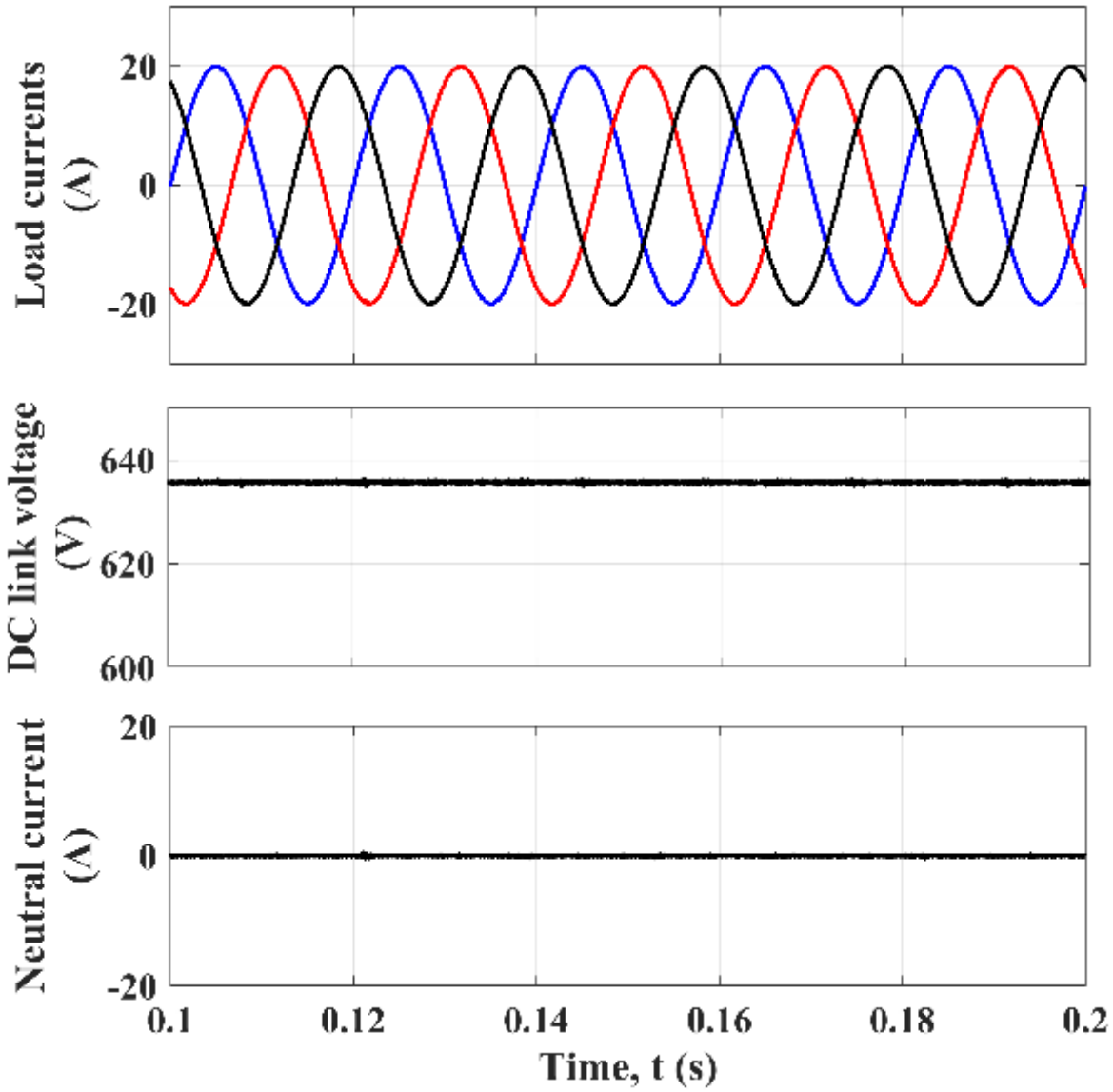

Fig. 4.2.With balanced references to the load current, a steady state is produced.

3-Balanced Resistance in transient mode R (R_1=R_2 =R_3)

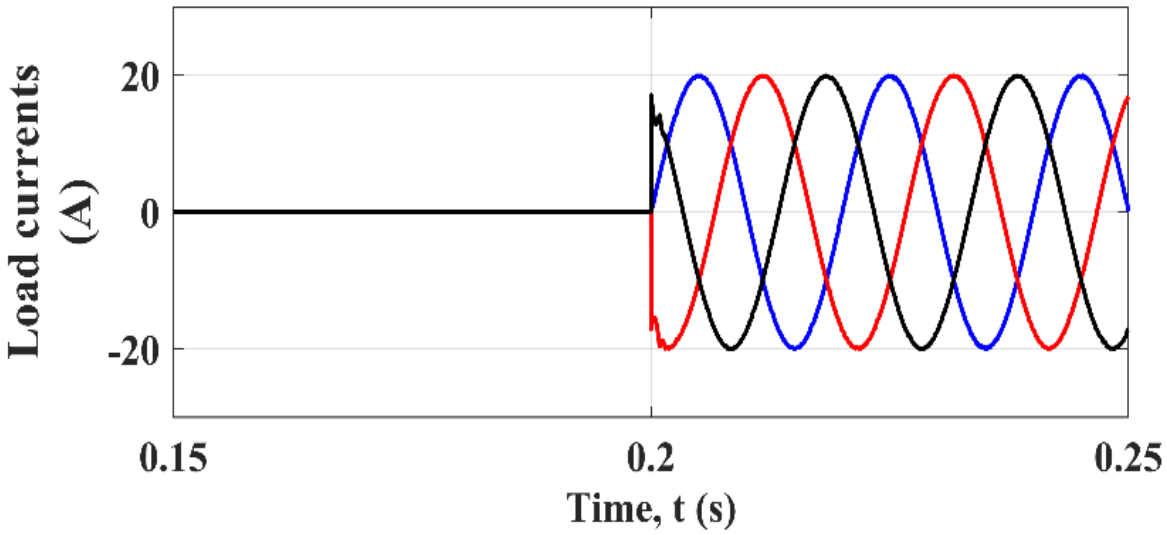

Fig. 4. 3.Load currents in Transient mode.

4.1.2.Case2 : Non Linear Loads

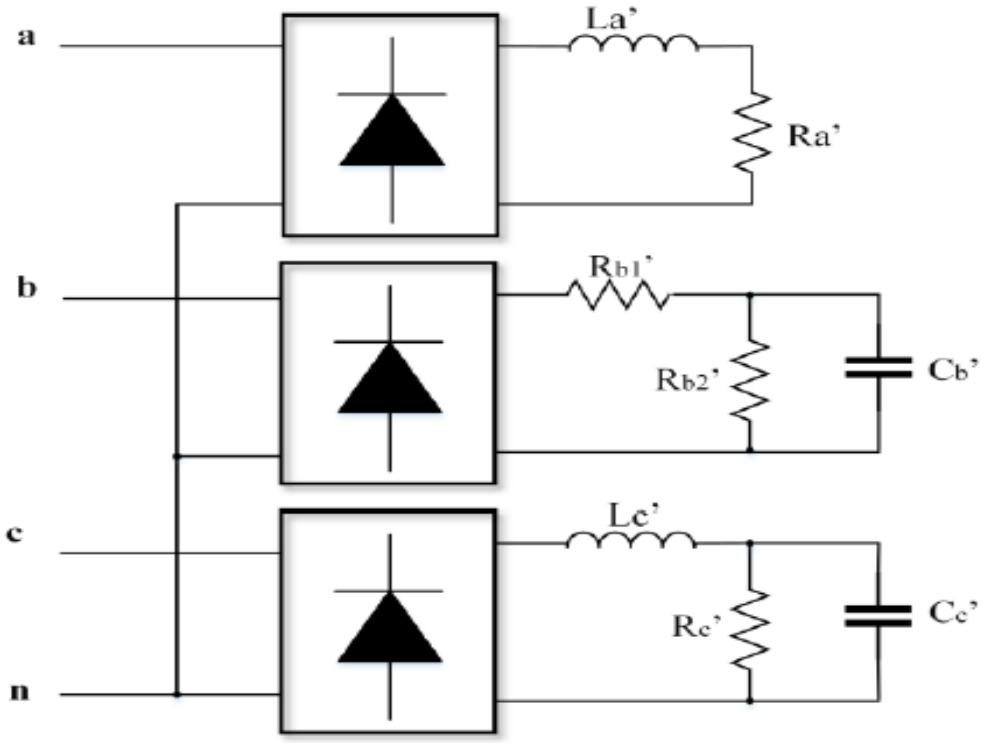

Fig. 4. 4. Three-phase nonlinear unbalanced loads' topology

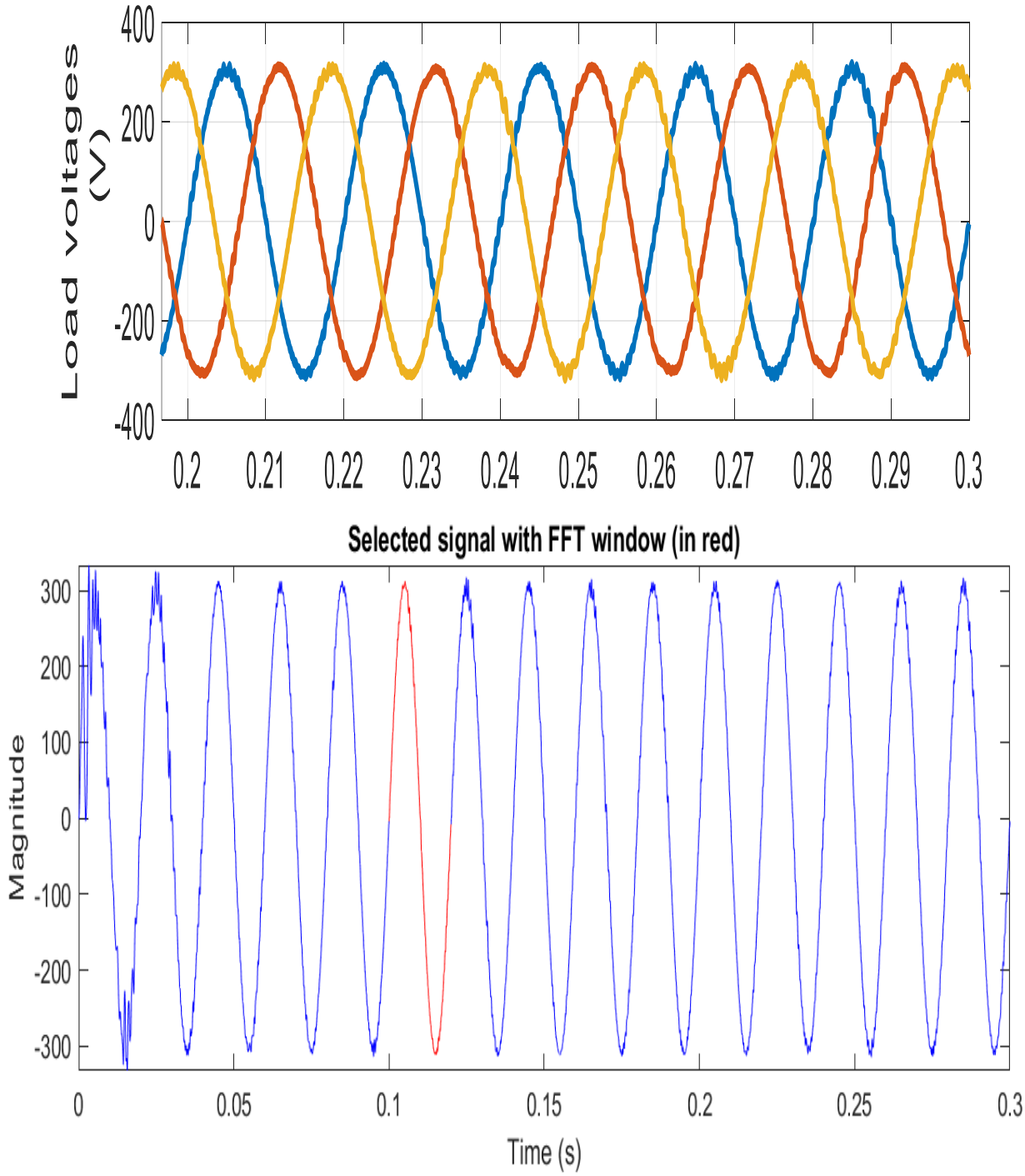

Fig. 4. 5. Loads Voltages.

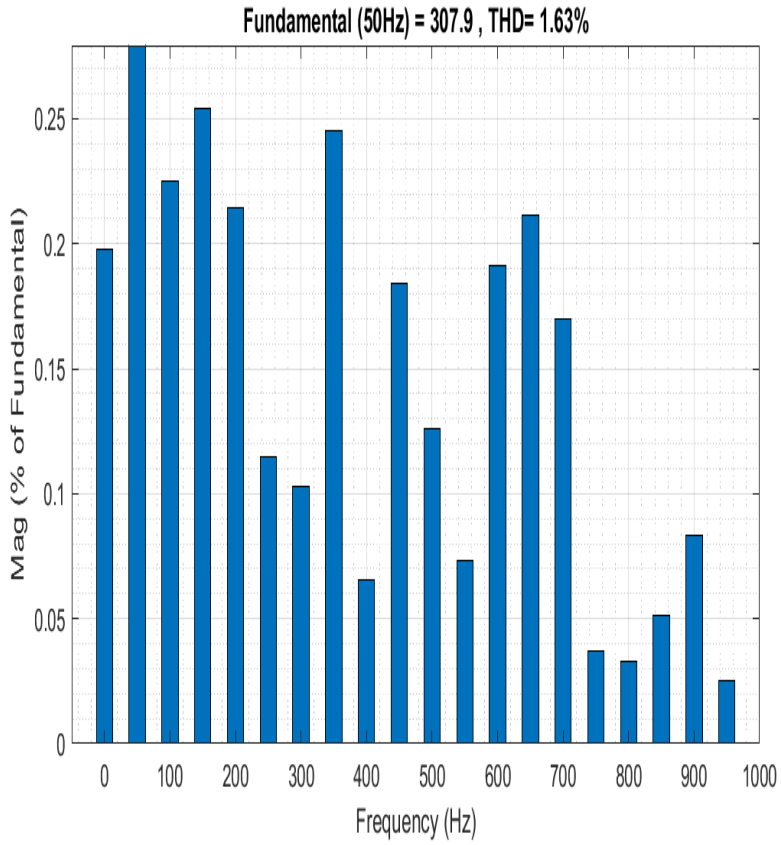

Sampling time	= 2e-05 sec.		
Samples per cycle	= 1000		
DC component	= 0.6099		
Fundamental	= 307.9 peak (217.7 rms)		
THD	= 1.63%		
0 Hz	DC	0.20%	270.0°
50 Hz	Fnd	100.00%	-0.2°
100 Hz	h2	0.23%	111.9°
150 Hz	h3	0.25%	268.1°
200 Hz	h4	0.21%	99.3°
250 Hz	h5	0.11%	-4.9°
300 Hz	h6	0.10%	265.9°
350 Hz	h7	0.24%	262.7°
400 Hz	h8	0.07%	14.9°
450 Hz	h9	0.18%	-29.7°
500 Hz	h10	0.13%	118.7°
550 Hz	h11	0.07%	182.6°

Fig. 4. 6. THD spectrum of the domestic voltage and the analysis of its harmonics.

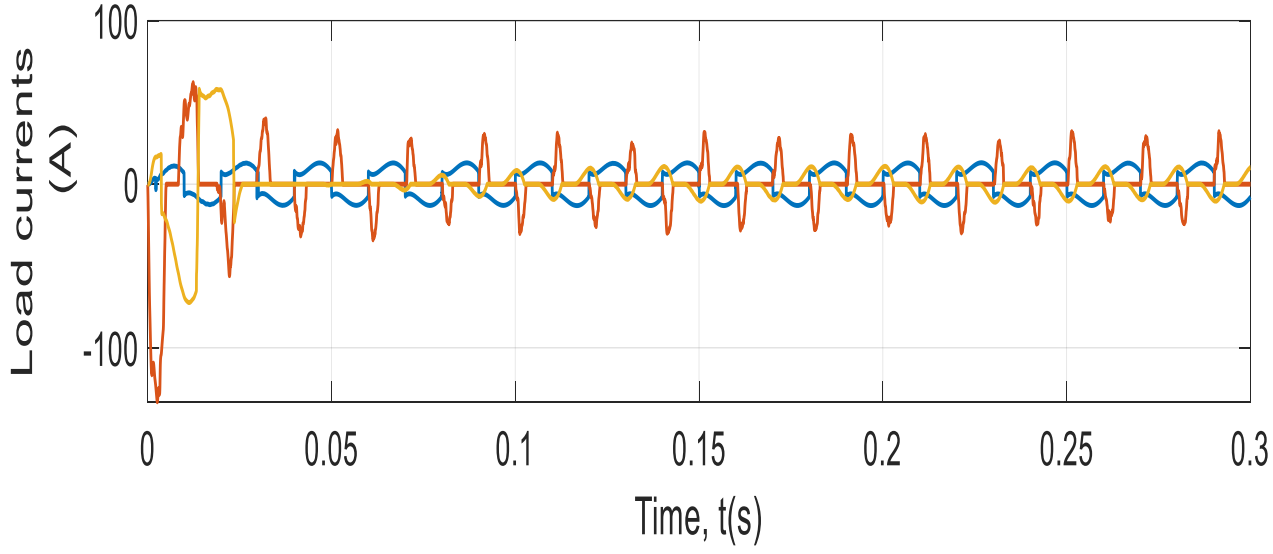

Fig. 4.7.Loads currents.

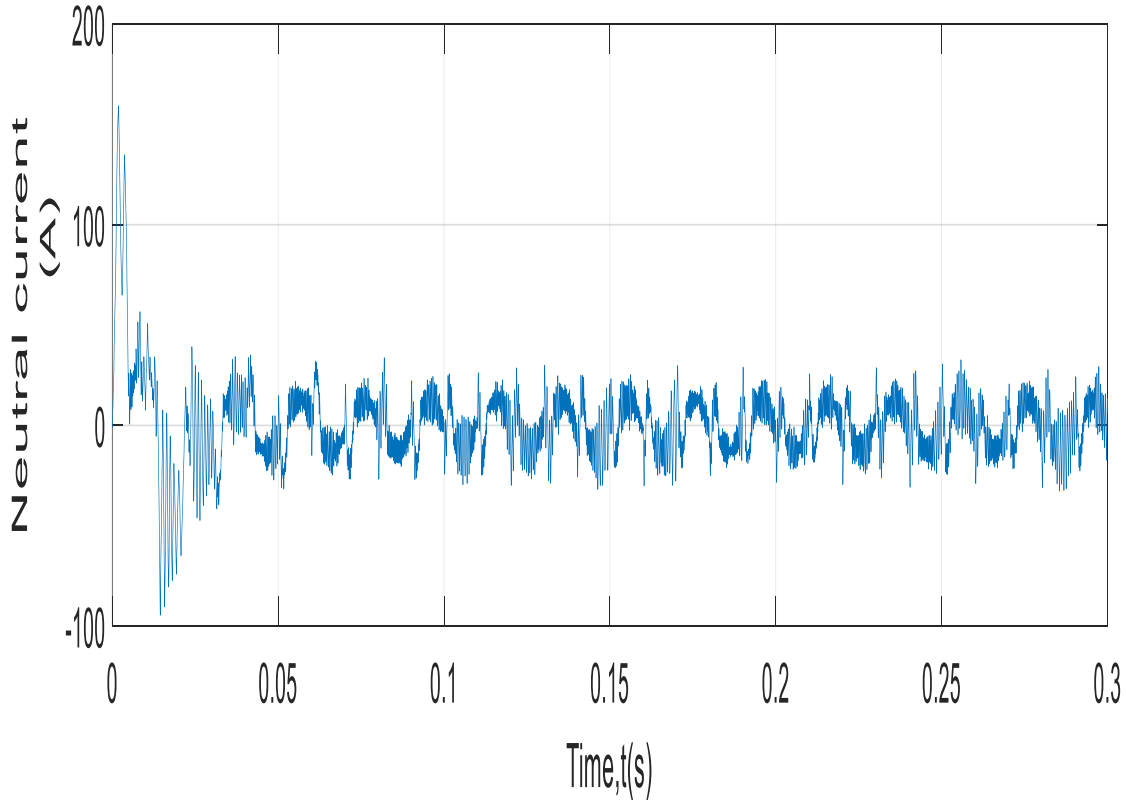

Fig. 4. 8. Neutral current.

Case 1:

There are three case studies carried out, two of which are in steady-state mode and one of which is in transient mode. When operating in steady-state modem, the proposed FSMPC is used to control the ZSFLI with unbalanced reference load currents (i_a= 60A, i_b= 25A, and i_c= 12A) in one case and balanced reference load currents (i_a= i_b=i_c = 20 A) in another case, with unbalanced load currents (R_a = 5Ω, R_b = 12Ω, and R_c = 25Ω) .Figures 4.1 and 4.2, which depict the results using unbalanced and balanced reference load currents, respectively. The results show that the proposed FSMPC algorithm can independently regulate each phase current while maintaining the same dc-link voltages. When the load currents are not balanced, the neutral current passes through the neutral wire.

The reference load currents are changed stepwise in transient mode from 0 to 20 A. Currents and loads for the reference load are balanced for this test (R_a=R_b=R_c=15 Ω). It can be seen from the results in Fig. 4.3 that the FSMPC control technique has a very quick transient reaction and a slight overshoot. Due to the balanced load current in this test, the neutral current is zero.

Case 2:

Three different nonlinear single phase loads in Fig. 4.4 illustrate how the system is connected to unbalanced nonlinear loads. The load voltage maintains sinusoidal and symmetrical characteristics with excellent reference voltage tracking, as shown by the results in Fig. 4.5. This outcome highlights MPC's capacity to handle non-linear loads. The load's voltage harmonic distortion does not exceed 4%, as shown in Fig. 4.6, and is therefore within acceptable bounds. According to Fig. 4.7, the load currents change depending on the overall load demand of each individual phase. Due to the nonlinearity of the load, as depicted in Fig. 4.8, the neutral current is essentially non-sinusoidal and travels along the fourth wire of the APS.

4.2. Conclusion

To test the dynamic and steady state performances of the described MPC scheme, simulation studies with a Z-source four leg inverter were conducted. According to simulation results, the described MPC technique offers simplicity and excellent control performance under a variety of reference current and load conditions.

GENERAL CONCLUSION

The finite control set model predictive control (FSMPC) algorithm for Z-source four-leg inverter (ZSFLI) current control in the electrical system is presented in this thesis. The primary benefit of using ZSFLI is to achieve single-stage power conversion for electrical systems with high controllability of unbalanced issues. The ZS network's load currents and capacitor voltage are controlled by the proposed FSMPC. Case studies were conducted to confirm the ZS inverter topology of the suggested control strategy's effectiveness. The outcomes demonstrate the excellent steady-state and transient performances of the suggested technique. A 4-leg Z-source inverter with an LC filter has its load voltages controlled using the FCS-MPC method. By reducing the number of mathematical operations while maintaining high control performance, the control algorithm is created to reduce the calculation time required for the implementation of a digital control system. The analysis's findings demonstrate that the suggested control algorithm provides high load voltage quality in the autonomous power supply (APS) with little total harmonic distortion (THD) when used under nonlinear and unbalanced load conditions. Furthermore, the control performance under varying loads shows strong static and dynamic responses.

Modern control theory and microprocessor advances have allowed for the using MPC in power electronics and drives in a natural and clear manner. MPC provides a high level of flexibility for controlling various circuit topologies and handling different control objectives without adding significant intricacy. MPC structure has several important advantages such as concepts are very intuitive and easy to understand, it can be applied to a great variety of systems, simple treatment of constraints, the resulting controller is easy to implement, obtain very fast transit response, the multivariable case can be easily considered. However, MPC structure

has also disadvantages like large number of calculations and the quality of the model have a direct influence of the quality of the resulting controller.

Appendix (A): Model Predictive control algorithm in Matlab

```
function [Vap,Vbp,Vcp] =
predictive_model(V_meas,I_o,I,v, Q, J)

Va = zeros(1,16);
Vb = zeros(1,16);
Vc = zeros(1,16);

% Read voltage measurements at sampling instant k
Vk = [V_meas(1) V_meas(2) V_meas(3)];
% Read output current  at sampling instant k
Iok = [I_o(1) I_o(2) I_o(3)];
% Read inverter current  at sampling instant k
Ik = [I(1) I(2) I(3)];

fori = 1:16
% calculate state variables from the discrete model
    STV = Q * [Vk'; Ik']+ J * [v(i,:)'; Iok'];
% calculate output predicted voltage
Ia(i) = STV(1);
Ib(i) = STV(2);
Ic(i) = STV(3);
end
Vap = Va;
Vbp = Vb;
Vcp = Vc;


function [Sa,Sb,Sc,Sn] = Obj_fn(Vref,Vap, Vbp, Vcp,
states)

g = zeros(1,16);  % Initialize the cost function

fori = 1:16

% Cost function
    g(i) = (Vref(1)-Vap(i))^2 + (Vref(2)-Vbp(i))^2+
(Vref(3)-Vcp(i))^2;
end
```

```
% Optimization
[~,x_opt] = min(g);

% Output switching states
Sa = states(x_opt,1);
Sb = states(x_opt,2);
Sc = states(x_opt,3);
Sn = states(x_opt,4);
```

References

[1] G. Zhang, Z. Li, B. Zhang, and W. A. Halang, "Power electronics converters: Past, present and future," *Renew. Sustain. Energy Rev.*, vol. 81, no. May, pp. 2028–2044, 2018, doi: 10.1016/j.rser.2017.05.290.

[2] A. Chatterjee and K. B. Mohanty, "Current control strategies for single phase grid integrated inverters for photovoltaic applications-a review," *Renew. Sustain. Energy Rev.*, vol. 92, no. April, pp. 554–569, 2018, doi: 10.1016/j.rser.2018.04.115.

[3] K. Zeb *et al.*, "A comprehensive review on inverter topologies and control strategies for grid connected photovoltaic system," *Renew. Sustain. Energy Rev.*, vol. 94, pp. 1120–1141, 2018, doi: 10.1016/j.rser.2018.06.053.

[4] X. Wang, J. M. Guerrero, F. Blaabjerg, and Z. Chen, "A review of power electronics based microgrids," *J. Power Electron.*, vol. 12, no. 1, pp. 181–192, 2012, doi: 10.6113/JPE.2012.12.1.181.

[5] R. Aboelsaud, A. Ibrahim, and A. G. Garganeev, "Review of three-phase inverters control for unbalanced load compensation," *Int. J. Power Electron. Drive Syst.*, vol. 10, no. 1, p. 242, 2019, doi: 10.11591/ijpeds.v10.i1.pp242-255.

[6] S. Obukhov, A. Ibrahim, A. A. Zaki Diab, A. S. Al-Sumaiti, and R. Aboelsaud, "Optimal Performance of Dynamic Particle Swarm Optimization Based Maximum Power Trackers for Standalone PV System under Partial Shading Conditions," *IEEE Access*, vol. 8, pp. 20770–20785, 2020, doi: 10.1109/ACCESS.2020.2966430.

[7] A. Ibrahim, R. Aboelsaud, and S. Obukhov, "Maximum power point tracking of partially shading PV system using cuckoo search algorithm," *Int. J. Power Electron. Drive Syst.*, vol. 10, no. 2, pp. 1081–1089, 2019, doi: 10.11591/ijpeds.v10.i2.pp1081-1089.

[8] R. Aboelsaud *et al.*, "Assessment of Model Predictive Voltage Control for Autonomous Four-Leg Inverter," *IEEE Access*, vol. 8, pp. 101163–101180, 2020, doi: 10.1109/ACCESS.2020.2996753.

[9] R. Aboelsaud, A. Ibrahim, and A. G. Garganeev, "Comparative Study Of Control Methods for Power Quality Improvement of Autonomous 4-Leg Inverters," *Proc. 1st IEEE 2019 Int. Youth Conf. Radio Electron. Electr. Power Eng. REEPE 2019*, pp. 1–6, 2019, doi: 10.1109/REEPE.2019.8708773.

[10] T. Li and Q. Cheng, "A comparative study of Z-source inverter and enhanced topologies," *CES Trans. Electr. Mach. Syst.*, vol. 2, no. 3, pp. 284–288, 2018, doi: 10.30941/cestems.2018.00035.

[11] Y. Liu, S. Member, B. Ge, H. Abu-rub, and S. Member, "Overview of Space Vector Modulations for Three- Phase Z-source / Quasi-Z-source Inverters," no. c.

[12] M. Hasan Babayi Nozadian, E. Babaei, S. H. Hosseini, and E. Shokati Asl, "Steady-State Analysis and Design Considerations of High Voltage Gain Switched Z-source Inverter with Continuous Input Current," *IEEE Trans. Ind. Electron.*, vol. 64, no. 7, pp. 5342–5350, 2017, doi: 10.1109/TIE.2017.2677315.

[13] Z. Yu, X. Hu, M. Zhang, L. Chen, and S. Jiang, "A transformerless boost inverter for standalone photovoltaic generation systems," *PEDG 2019 - 2019 IEEE 10th Int. Symp. Power Electron. Distrib. Gener. Syst.*, pp. 570–575, 2019, doi: 10.1109/PEDG.2019.8807688.

[14] S. A. Singh, G. Carli, N. A. Azeez, and S. S. Williamson, "Modeling, Design, Control, and Implementation of a Modified Z-source Integrated PV/Grid/EV DC Charger/Inverter," *IEEE Trans. Ind. Electron.*, vol. 65, no. 6, pp. 5213–5220, 2018, doi: 10.1109/TIE.2017.2784396.

[15] J. Liu, J. Wu, J. Qiu, and J. Zeng, "Switched Z-source/Quasi-Z-source DC-DC converters with reduced passive components for photovoltaic systems," *IEEE Access*, vol. 7, pp. 40893–40903, 2019, doi: 10.1109/ACCESS.2019.2907300.

[16] V. Yaramasu, M. Rivera, B. Wu, and J. Rodriguez, "Predictive control of four-leg power converters," *Proc. - 2015 IEEE Int. Symp. Predict. Control Electr. Drives Power Electron. Preced. 2015*, no. October, pp. 121–125, 2016, doi: 10.1109/PRECEDE.2015.7395594.

[17] X. Guo, Y. Yang, R. He, B. Wang, and F. Blaabjerg, "Transformerless Z-source Four-Leg PV Inverter with Leakage Current Reduction," *IEEE Trans. Power Electron.*, vol. 34, no. 5, pp. 4343–4352, 2019, doi: 10.1109/TPEL.2018.2861896.

[18] Y. Han, A. T. Jiang, E. A. A. Coelho, and J. M. Guerrero, "Optimal Performance Design Guideline of Hybrid Reference Frame Based Dual-Loop Control Strategy for Standalone Single-Phase Inverters," *IEEE Trans. Energy Convers.*, vol. 33, no. 2, pp. 730–740, 2018, doi: 10.1109/TEC.2017.2769114.

[19] X. Wang, Y. Lin, B. Wang, W. Liu, and K. Bai, "Output Voltage Control of BESS Inverter in Standalone Micro-Grid Based on Expanded Inverse Model," *IEEE Access*, vol. 8, pp. 3781–3791, 2020, doi: 10.1109/ACCESS.2019.2962530.

[20] S. Bayhan, M. Trabelsi, H. Abu-Rub, and M. Malinowski, "Finite-Control-Set Model-Predictive Control for a Quasi-Z-source Four-Leg Inverter Under Unbalanced Load Condition," *IEEE Trans. Ind. Electron.*, vol. 64, no. 4, pp. 2560–2569, 2017, doi: 10.1109/TIE.2016.2632062.

[21] P. Basak, S. Chowdhury, S. Halder Nee Dey, and S. P. Chowdhury, "A literature review on integration of distributed energy resources in the perspective of control, protection and stability of microgrid," *Renew. Sustain. Energy Rev.*, vol. 16, no. 8, pp. 5545–5556, 2012, doi: 10.1016/j.rser.2012.05.043.

[22] D. E. Olivares *et al.*, "Trends in microgrid control," *IEEE Trans. Smart Grid*, vol. 5, no. 4, pp. 1905–1919, 2014, doi: 10.1109/TSG.2013.2295514.

[23] R. Zamora and A. K. Srivastava, "Controls for microgrids with storage: Review, challenges, and research needs," *Renew. Sustain. Energy Rev.*, vol. 14, no. 7, pp. 2009–2018, 2010, doi: 10.1016/j.rser.2010.03.019.

[24] O. Palizban and K. Kauhaniemi, "Hierarchical control structure in microgrids with distributed generation: Island and grid-connected mode," *Renew. Sustain. Energy Rev.*, vol. 44, pp. 797–813, 2015, doi: 10.1016/j.rser.2015.01.008.

[25] T. L. Vandoorn, J. D. M. De Kooning, B. Meersman, and L. Vandevelde, "Review of primary control strategies for islanded microgrids with power-electronic interfaces," *Renew. Sustain. Energy Rev.*, vol. 19, pp. 613–628, 2013, doi: 10.1016/j.rser.2012.11.062.

[26] M. Soshinskaya, W. H. J. Crijns-Graus, J. M. Guerrero, and J. C. Vasquez, "Microgrids: Experiences, barriers and success factors," *Renew. Sustain. Energy Rev.*, vol. 40, pp. 659–672, 2014, doi: 10.1016/j.rser.2014.07.198.

[27] N. Hatziargyriou, H. Asano, R. Iravani, and C. Marnay, "Microgrids," *IEEE Power Energy Mag.*, vol. 5, no. 4, pp. 78–94, 2007, doi: 10.1109/MPAE.2007.376583.

[28] P. G. Arul, V. K. Ramachandaramurthy, and R. K. Rajkumar, "Control strategies for a hybrid renewable energy system: A review," *Renew. Sustain. Energy Rev.*, vol. 42, pp. 597–608, 2015, doi: 10.1016/j.rser.2014.10.062.

[29] A. Mohd, E. Ortjohann, D. Morton, and O. Omari, "Review of control techniques for inverters parallel operation," *Electr. Power Syst. Res.*, vol. 80, no. 12, pp. 1477–1487, 2010, doi: 10.1016/j.epsr.2010.06.009.

[30] S. B. and B. Chowdhury, "Hybrid AC / DC Power Distribution Solution for Future Space Applications," *Proc. IEEE PESGM*, vol. 65401, pp. 1–8, 2007.

[31] Z. Jiang and X. Yu, "Hybrid DC- and AC-linked microgrids: Towards integration of distributed energy resources," *2008 IEEE Energy 2030 Conf. ENERGY 2008*, 2008, doi: 10.1109/ENERGY.2008.4781029.

[32] and A. D. F. Katiraei, R. Iravani, N. Hatziargyriou, "Microgrids management," *IEEE Power Energy Mag.*, vol. 6, no. june, pp. 54–65, 2008.

[33] Z. Chen, J. M. Guerrero, F. Blaabjerg, and S. Member, "A Review of the State of the Art of Power Electronics for Wind Turbines," *IEEE Trans. Power Electron.*, vol. 24, no. 8, pp. 1859–1875, 2009, doi: 10.1109/TPEL.2009.2017082.

[34] B. Meersman, B. Renders, L. Degroote, T. Vandoorn, J. De Kooning, and L. Vandevelde, "Overview of three?phase inverter topologies for distributed generation purposes," *i?SUP 2010 Innov. Sustain. Prod. Proc.*, p. 24??28, 2010.

[35] M. N. Marwali and A. Keyhani, "Control of distributed generation systems - Part I: Voltages and currents control," *IEEE Trans. Power Electron.*, vol. 19, no. 6, pp. 1541–1550, 2004, doi: 10.1109/TPEL.2004.836685.

[36] L. Peng, D. Bai, Y. Kang, and J. Chen, "Research on three-phase inverter with unbalanced

load," *Zhongguo Dianji Gongcheng Xuebao/Proceedings Chinese Soc. Electr. Eng.*, vol. 24, no. 5, pp. 174–178, 2004, doi: 10.1109/apec.2004.1295799.

[37] D. Soto, C. Edrington, S. Balathandayuthapani, and S. Ryster, "Voltage balancing of islanded microgrids using a time-domain technique," *Electr. Power Syst. Res.*, vol. 84, no. 1, pp. 214–223, 2012, doi: 10.1016/j.epsr.2011.11.022.

[38] P. K. Goel, B. Singh, S. S. Murthy, and N. Kishore, "Isolated wind-hydro hybrid system using cage generators and battery storage," *IEEE Trans. Ind. Electron.*, vol. 58, no. 4, pp. 1141–1153, 2011, doi: 10.1109/TIE.2009.2037646.

[39] M. R. Miveh, M. F. Rahmat, A. A. Ghadimi, and M. W. Mustafa, "Control techniqWues for three-phase foWur-leg voltage soWurce inverters in aWutonomoWus microgrids: A review," *Renew. Sustain. Energy Rev.*, vol. 54, pp. 1592–1610, 2016, doi: 10.1016/j.rser.2015.10.079.

[40] A. Hintz, U. R. Prasanna, and K. Rajashekara, "Comparative Study of the Three-Phase Grid-Connected Inverter Sharing Unbalanced Three-Phase and/or Single-Phase systems," *IEEE Trans. Ind. Appl.*, vol. 52, no. 6, pp. 5156–5164, 2016, doi: 10.1109/TIA.2016.2593680.

[41] J. Liang, T. C. Green, C. Feng, and G. Weiss, "Increasing voltage utilization in split-link, four-wire inverters," *IEEE Trans. Power Electron.*, vol. 24, no. 6, pp. 1562–1569, 2009, doi: 10.1109/TPEL.2009.2013351.

[42] M. K. Mishra, A. Joshi, and A. Ghosh, "Control schemes for equalization of capacitor voltages in neutral clamped shunt compensator," *IEEE Trans. Power Deliv.*, vol. 18, no. 2, pp. 538–544, 2003, doi: 10.1109/TPWRD.2003.809684.

[43] P. Lohia, M. K. Mishra, K. Karthikeyan, and K. Vasudevan, "A minimally switched control algorithm for three-phase four-leg VSI topology to compensate unbalanced and non-linear load," *IEEE Trans. Power Electron.*, vol. 23, no. 4, pp. 1935–1944, 2008, doi: 10.1109/TPEL.2008.925414.

[44] R. Zhang, V. H. Prasad, D. Boroyevich, and F. C. Lee, "Three-dimensional space vector modulation for four-leg voltage-source converters," *IEEE Trans. Power Electron.*, vol. 17, no. 3, pp. 314–326, 2002, doi: 10.1109/TPEL.2002.1004239.

[45] C. L. Chen and C. E. Lin, "An active filter for an unbalanced three-phase system using the synchronous detection method," *Electr. Power Syst. Res.*, vol. 36, no. 3, pp. 157–161, 1996, doi: 10.1016/0378-7796(95)01026-2.

[46] V. Khadkikar and A. Chandra, "An independent control approach for three-phase four-wire shunt active filter based on three H-bridge topology under unbalanced load conditions," *PESC Rec. - IEEE Annu. Power Electron. Spec. Conf.*, pp. 4643–4649, 2008, doi: 10.1109/PESC.2008.4592699.

[47] W. Qian, F. Z. Peng, and H. Cha, "Trans-Z-source Inverters," vol. 26, no. 12, pp. 3453–3463, 2011.

[48] P. D. F. Pack, I. Transact, I. A. S. A. Meet, and C. Rec, “Z-source Inverter Z-source Inverter,” 2002.

[49] S. Bayhan, M. Trabelsi, and H. Abu-Rub, “Model Predictive Control of Z-source four-leg inverter for standalone Photovoltaic system with unbalanced load,” *Conf. Proc. - IEEE Appl. Power Electron. Conf. Expo. - APEC*, vol. 2016-May, pp. 3663–3668, 2016, doi: 10.1109/APEC.2016.7468397.

[50] E. C. Dos Santos, J. H. G. Muniz, E. P. X. P. Filho, and E. R. C. Da Silva, “Dc-ac three-phase four-wire Z-source converter with hybrid PWM strategy,” *IECON Proc. (Industrial Electron. Conf.*, pp. 409–414, 2010, doi: 10.1109/IECON.2010.5674993.

[51] Y. Tang, S. Xie, C. Zhang, and Z. Xu, “Improved Z-source inverter with reduced Z-source capacitor voltage stress and soft-start capability,” *IEEE Trans. Power Electron.*, vol. 24, no. 2, pp. 409–415, 2009, doi: 10.1109/TPEL.2008.2006173.

[52] M. M. Hussein, T. Senjyu, M. Orabi, M. A. A. Wahab, and M. M. Hamada, “Control of a standalone variable speed wind energy supply system,” *Appl. Sci.*, vol. 3, no. 2, pp. 437–456, 2013, doi: 10.3390/app3020437.

[53] R. Cárdenas, R. Peña, J. Clare, P. Wheeler, and P. Zanchetta, “A repetitive control system for four-leg matrix converters feeding non-linear loads,” *Electr. Power Syst. Res.*, vol. 104, pp. 18–27, 2013, doi: 10.1016/j.epsr.2013.05.012.

[54] R. Cárdenas, R. Peña, P. Wheeler, J. Clare, and C. Juri, “Control of a matrix converter for the operation of autonomous systems,” *Renew. Energy*, vol. 43, pp. 343–353, 2012, doi: 10.1016/j.renene.2011.11.052.

[55] M. Matteini, “Control Techniques for Matrix Conv Adjustable Speed Drives,” *PhD Thesis*, vol. 7, pp. 1998–2001, 2001.

[56] T. Friedli, J. W. Kolar, J. Rodriguez, and P. W. Wheeler, “Comparative evaluation of three-phase AC-AC matrix converter and voltage DC-link back-to-back converter systems,” *IEEE Trans. Ind. Electron.*, vol. 59, no. 12, pp. 4487–4510, 2012, doi: 10.1109/TIE.2011.2179278.

[57] R. Aboelsaud, A. Ibrahim, and A. G. Garganeev, “Voltage Control of Autonomous Power Supply Systems Based on PID Controller Under Unbalanced and Nonlinear Load Conditions,” *Proc. 1st IEEE 2019 Int. Youth Conf. Radio Electron. Electr. Power Eng. REEPE 2019*, pp. 1–6, 2019, doi: 10.1109/REEPE.2019.8708841.

[58] Y. Bomstein *et al.*, *The antiapoptotic effects of blood constituents in patients with chronic lymphocytic leukemia*, vol. 70, no. 5. 2003.

[59] J. G. Hwang, P. W. Lehn, and M. Winkelnkemper, “A generalized class of stationary frame-current controllers for grid-connected ACDC converters,” *IEEE Trans. Power Deliv.*, vol. 25, no. 4, pp. 2742–2751, 2010, doi: 10.1109/TPWRD.2010.2045136.

[60] G. Shen, X. Zhu, J. Zhang, and D. Xu, “A new feedback method for PR current control of LCL-filter-based grid-connected inverter,” *IEEE Trans. Ind. Electron.*, vol. 57, no. 6, pp.

2033–2041, 2010, doi: 10.1109/TIE.2010.2040552.

[61] Novosibirskiĭ gosudarstvennyĭ tekhnicheskiĭ universitet, Institute of Electrical and Electronics Engineers. Russia Siberia Section, and Institute of Electrical and Electronics Engineers, "2019 20th International Conference of Young Specialists on Micro/Nanotechnologies and Electron Devices : proceedings : Erlagol, Altai Republic, 29 June -3 July, 2019," *2019 20th Int. Conf. Young Spec. Micro/Nanotechnologies Electron Devices*, pp. 558–564, 2019.

[62] G. Zames, "Feedback and Optimal Sensitivity: Model Reference Transformations, Multiplicative Seminorms, and Approximate Inverses," *IEEE Trans. Automat. Contr.*, vol. 26, no. 2, pp. 301–320, 1981, doi: 10.1109/TAC.1981.1102603.

[63] T. Hornik and Q. C. Zhong, "A current-control strategy for voltage-source inverters in microgrids based on H∞ and Repetitive Control," *IEEE Trans. Power Electron.*, vol. 26, no. 3, pp. 943–952, 2011, doi: 10.1109/TPEL.2010.2089471.

[64] S. Yang, Q. Lei, F. Z. Peng, and Z. Qian, "A robust control scheme for grid-connected voltage-source inverters," *IEEE Trans. Ind. Electron.*, vol. 58, no. 1, pp. 202–212, 2011, doi: 10.1109/TIE.2010.2045998.

[65] M. Chhabra and F. Barnes, "Robust current controller design using mu-synthesis for grid-connected three phase inverter," *2014 IEEE 40th Photovolt. Spec. Conf. PVSC 2014*, pp. 1413–1418, 2014, doi: 10.1109/PVSC.2014.6925182.

[66] T. Hornik and Q. C. Zhong, "H∞ repetitive current controller for grid-connected inverters," *IECON Proc. (Industrial Electron. Conf.*, pp. 554–559, 2009, doi: 10.1109/IECON.2009.5414981.

[67] H. Komurcugil, "Rotating-sliding-line-based sliding-mode control for single-phase UPS inverters," *IEEE Trans. Ind. Electron.*, vol. 59, no. 10, pp. 3719–3726, 2012, doi: 10.1109/TIE.2011.2159354.

[68] S. Yarahmadi, G. A. Markade, and J. Soltani, "Current harmonics reduction of non-linear load by using active power filter based on improved sliding mode control," *PEDSTC 2013 - 4th Annu. Int. Power Electron. Drive Syst. Technol. Conf.*, pp. 524–528, 2013, doi: 10.1109/PEDSTC.2013.6506763.

[69] Y. Sun, M. Qian, Y. Lin, and Z. Bai, "A fuzzy-sliding mode controller for four-quadrant PWM converter of grid-connected wind generation simulator," *2011 Int. Conf. Consum. Electron. Commun. Networks, CECNet 2011 - Proc.*, pp. 3827–3830, 2011, doi: 10.1109/CECNET.2011.5768493.

[70] B. Bouaziz and F. Bacha, "Direct power control of grid-connected converters using sliding mode controller," *2013 Int. Conf. Electr. Eng. Softw. Appl. ICEESA 2013*, no. July 2015, 2013, doi: 10.1109/ICEESA.2013.6578497.

[71] X. Hao, T. Liu, X. Yang, and L. Huang, "A discrete-time integral sliding-mode controller with nonlinearity compensation for three-phase grid-connected photovoltaic inverter,"

Conf. Proc. - 2012 IEEE 7th Int. Power Electron. Motion Control Conf. - ECCE Asia, IPEMC 2012, vol. 2, pp. 831–835, 2012, doi: 10.1109/IPEMC.2012.6258953.

[72] N. Kumar, T. K. Saha, and J. Dey, "Sliding-Mode Control of PWM Dual Inverter-Based Grid-Connected PV System: Modeling and Performance Analysis," *IEEE J. Emerg. Sel. Top. Power Electron.*, vol. 4, no. 2, pp. 435–444, 2016, doi: 10.1109/JESTPE.2015.2497900.

[73] Y. Thiagarajan, T. S. Sivakumaran, and P. Sanjeevikumar, "Design and simulation of fuzzy controller for a grid connected stand alone PV system," *Proc. 2008 Int. Conf. Comput. Commun. Networking, ICCCN 2008*, no. May 2014, 2008, doi: 10.1109/ICCCNET.2008.4787740.

[74] N. G. M. Thao, M. T. Dat, T. C. Binh, and N. H. Phuc, "PID-fuzzy logic hybrid controller for grid-connected photovoltaic inverters," *2010 Int. Forum Strateg. Technol. IFOST 2010*, no. August 2015, pp. 140–144, 2010, doi: 10.1109/IFOST.2010.5668024.

[75] R. Zhao, Z. Chang, P. Yuan, L. Yang, and Z. Li, "A novel fuzzy logic and anti-windup PI controller for three-phase grid connected inverter," *PEITS 2009 - 2009 2nd Conf. Power Electron. Intell. Transp. Syst.*, vol. 1, pp. 442–446, 2009, doi: 10.1109/PEITS.2009.5406975.

[76] H. Shareef, A. Mohamed, and A. H. Mutlag, "A current control strategy for a grid connected PV system using fuzzy logic controller," *Proc. IEEE Int. Conf. Ind. Technol.*, pp. 890–894, 2014, doi: 10.1109/ICIT.2014.6894948.

[77] S. G. Thakare, H. S. Dalvi, and K. D. Joshi, "Statcom based fuzzy controller for grid connected wind generator," *2009 2nd Int. Conf. Emerg. Trends Eng. Technol. ICETET 2009*, pp. 35–39, 2009, doi: 10.1109/ICETET.2009.212.

[78] I. Applications and P. Electronics, "Model predictive control review its applications powerelectronics."

[79] S. Vazquez, J. Rodriguez, M. Rivera, L. G. Franquelo, and M. Norambuena, "Model Predictive Control for Power Converters and Drives: Advances and Trends," *IEEE Trans. Ind. Electron.*, vol. 64, no. 2, pp. 935–947, 2017, doi: 10.1109/TIE.2016.2625238.

[80] V. Yaramasu, M. Rivera, M. Narimani, B. Wu, and J. Rodriguez, "Model predictive approach for a simple and effective load voltage control of four-leg inverter with an output LC filter," *IEEE Trans. Ind. Electron.*, vol. 61, no. 10, pp. 5259–5270, 2014, doi: 10.1109/TIE.2013.2297291.

[81] A. Yazdani *et al.*, "Modeling guidelines and a benchmark for power system simulation studies of three-phase single-stage photovoltaic systems," *IEEE Trans. Power Deliv.*, vol. 26, no. 2, pp. 1247–1264, 2011, doi: 10.1109/TPWRD.2010.2084599.

[82] P. C. Loh, D. M. Vilathgamuwa, Y. Sen Lai, G. T. Chua, and Y. Li, "Pulse-width modulation of Z-source inverters," *Conf. Rec. - IAS Annu. Meet. (IEEE Ind. Appl. Soc.*, vol. 1, pp. 148–155, 2004, doi: 10.1109/ias.2004.1348401.

[83] I. Quiros, “Thick DGP braneworlds: Geometrical origin of inflation and of present acceleration of the expansion,” *AIP Conf. Proc.*, vol. 1083, no. 4, pp. 182–189, 2008, doi: 10.1063/1.3058566.

[84] E. Twining and D. G. Holmes, “Grid current regulation of a three-phase voltage source inverter with an LCL input filter,” *IEEE Trans. Power Electron.*, vol. 18, no. 3, pp. 888–895, 2003, doi: 10.1109/TPEL.2003.810838.

[85] A. Teta, “A Survey on modulation approaches for Z-source inverter,” no. February, pp. 1–5, 2019.

[86] K. Zeb *et al.*, “A comprehensive review on inverter topologies and control strategies for grid connected photovoltaic system,” *Renew. Sustain. Energy Rev.*, vol. 94, no. July, pp. 1120–1141, 2018, doi: 10.1016/j.rser.2018.06.053.

[87] T. Nguyen-Van and N. Hori, “New class of discrete-time models for non-linear systems through discretisation of integration gains,” *IET Control Theory Appl.*, vol. 7, no. 1, pp. 80–89, 2013, doi: 10.1049/iet-cta.2012.0010.

[88] J. Rodriguez and P. Cortes, *Predictive Control of Power Converters and Electrical Drives*. 2012.

[89] M. T. Boussabeur *et al.*, “Current control of Z-source four-leg inverter for autonomous photovoltaic system based on model predictive control,” *Bull. Tomsk Polytech. Univ. Geo Assets Eng.*, vol. 332, no. 7, pp. 165–171, 2021, doi: 10.18799/24131830/2021/7/3280.

Abstract

Due to geo-reasons like the low generation cost and clean energy resources, renewable energy sources have attracted more interest than the conventional underground fuels for the generation of electrical power. Furthermore, consumers who are geographically located in remote, inhospitable areas can effectively use renewable energy resources, particularly photovoltaic generation systems, as a self-sufficient power supply. The conversion system and its control method play a major role in the performance of the autonomous power supply. In order to control the load current of the Z-source four-leg inverter used for electrical system, this thesis uses a modern and alternative control system based on the finite control set model predictive control strategy.

Key words
Renewable energy resources, electrical systems, model predictive control, four-leg inverter, Z-source inverter.

Résumé

Pour des raisons géographiques telles que le faible coût de production et les ressources énergétiques propres, les sources d'énergie renouvelables ont suscité plus d'intérêt que les combustibles souterrains conventionnels pour la production d'énergie électrique. En outre, les consommateurs qui se trouvent géographiquement dans des zones reculées et inhospitalières peuvent utiliser efficacement les ressources énergétiques renouvelables, en particulier les systèmes de production photovoltaïque, comme source d'énergie autosuffisante. Le système de conversion et sa méthode de contrôle jouent un rôle majeur dans les performances de l'alimentation électrique autonome. Afin de contrôler le courant de charge de l'onduleur Z source à quatre bras utilisé pour le système électrique, cette thèse utilise un moderne système de contrôle alternatif basé sur la stratégie de contrôle prédictif du modèle d'ensemble de contrôle fini.

Mots clés

Ressources énergétiques renouvelables, systèmes électriques, contrôle prédictif du modèle, onduleur à quatre bras, onduleur à Z- source.

ملخص

نظرا لأسباب جغرافية مثل انخفاض تكلفة التوليد وموارد الطاقة النظيفة، جذبت مصادر الطاقة المتجددة اهتماما أكبر من الوقود التقليدي تحت الأرض لتوليد الطاقة الكهربائية. علاوة على ذلك ، يمكن للمستهلكين الموجودين جغرافيا في مناطق نائية وغير مضيافة استخدام موارد الطاقة المتجددة بشكل فعال ، وخاصة أنظمة توليد الطاقة الكهروضوئية ، كمصدر طاقة مكتف ذاتيا. يلعب نظام التحويل وطريقة التحكم الخاصة به دورا رئيسيا في أداء مصدر الطاقة المستقل. من أجل التحكم في تيار الحمل للعاكس رباعي الأرجل زاد سورس المستخدم في النظام الكهربائي ، تستخدم هذه الأطروحة نظام تحكم حديث وبديل يعتمد على إستراتيجية التحكم التنبؤية لنموذج مجموعة التحكم المحدودة.

الكلمات الرئيسية
موارد الطاقة المتجددة ، الأنظمة الكهربائية ، التحكم في النموذج التنبؤي ، العاكس بأربعة أذرع ، العاكس.